

# 1 Annual high-resolution grazing intensity maps on the 2 Qinghai-Tibet Plateau from 1990 to 2020

3 Jia Zhou<sup>1,2</sup>, Jin Niu<sup>3</sup>, Ning Wu<sup>1</sup>, Tao Lu<sup>1\*</sup>

4 <sup>1</sup>Chengdu Institute of Biology, Chinese Academy of Sciences, Chengdu 610213, China

5 <sup>2</sup>University of Chinese Academy of Sciences, Beijing 100049, China

6 <sup>3</sup>Department of Economics, Brown University, Providence, 02912, USA

7 *Correspondence to:* Tao Lu ([lutao@cib.ac.cn](mailto:lutao@cib.ac.cn))

8 **Abstract.** Grazing activities constitute the paramount challenge to grassland conservation over the  
9 Qinghai-Tibet Plateau (QTP), underscoring the urgency for obtaining detailed extent, patterns, and  
10 trends of grazing information to access efficient grassland management and sustainable development.  
11 Here, to inform these issues, we provided the first annual Gridded Dataset of Grazing Intensity maps  
12 (GDGI) with a resolution of 100 meters from 1990 to 2020 for the QTP. Five most commonly used  
13 machine learning algorithms were leveraged to develop livestock spatialization model, which spatially  
14 disaggregate the livestock census data at the county level into a detailed 100 m× 100 m grid, based on  
15 seven key predictors from terrain, climate, vegetation and socio-economic factors. Among these  
16 algorithms, the extreme trees (ET) model performed the best in representing the complex nonlinear  
17 relationship between various environmental factors and livestock intensity, with an average absolute  
18 error of just 0.081 SU/hm<sup>2</sup>, a rate outperforming the other models by 21.58%~414.60%. By using the  
19 ET model, we further generated the GDGI dataset for the QTP to reveal the spatio-temporal  
20 heterogeneity and variation in grazing intensities. The GDGI indicates grazing intensity remained high  
21 and largely stable from 1990 to 1997, followed by a sharp decline from 1997 to 2001, and fluctuated  
22 thereafter. Encouragingly, comparing with other open-access datasets for grazing distribution on the  
23 QTP, the GDGI has the highest accuracy, with the determinant coefficient ( $R^2$ ) exceed 0.8. Given its  
24 high resolution, recentness and robustness, we believe that the GDGI dataset can significantly enhance  
25 understanding of the substantial threats to grasslands emanating from overgrazing activities.  
26 Furthermore, the GDGI product holds considerable potential as a foundational source for other  
27 researches, facilitating rational utilization of grasslands, refined environmental impact assessments, and  
28 the sustainable development of animal husbandry. The GDGI product developed in this study is  
29 available at <https://doi.org/10.5281/zenodo.10851119> (Zhou et al., 2024).

## 30 **1 Introduction**

31 Livestock is a crucial contributor to global food systems through the provision of essential animal  
32 proteins and fats, and plays a significant role in supporting human survival and socio-economic  
33 development (Gilbert et al., 2018; Godfray et al., 2018; Humpenöder et al., 2022; Kumar et al., 2022).  
34 However, the escalating increase in human demand for meat and dairy products over recent decades has  
35 triggered a livestock boom, which in turn has increasingly threatened grassland ecosystems and placed  
36 a heavy burden on the environment through overgrazing and land-use change (Tabassum et al., 2016;  
37 Wei et al., 2022; Minoofar et al., 2023). It is estimated that up to 300 million hectares of land are used  
38 globally for grazing and cultivating fodder crops (Tabassum et al., 2016). Grazing activities could alter  
39 vegetation phenology and community structure (Dong et al., 2020), and trigger deforestation (García  
40 Ruiz et al., 2020), grassland degradation (Sun et al., 2020), soil erosion (Shakoor et al., 2021), and  
41 associated direct releases in greenhouse gas that lead to climate change feedback (Godfray et al., 2018;  
42 Chang et al., 2021). Additionally, livestock are responsible for large-scale dispersion of pathogens,  
43 organic matter, and residual medications into soil and groundwater, thereby contaminating the  
44 environment (Venglovsky et al., 2009; Tabassum et al., 2016; Hu et al., 2017; Muloi et al., 2022).  
45 Consequently, more and more scholars have called attention to provide reliable contemporary dataset to  
46 illustrate the spatio-temporal heterogeneity and variation of livestock (Petz et al., 2014; Fetzel et al.,  
47 2017; Zhang et al., 2018; Li et al., 2021).

48 One of the major challenges in monitoring grazing activity at regional or even larger scale, is the  
49 determination of the livestock distribution pattern. Despite the importance of geographical grazing  
50 information, high spatio-temporal grazing dataset remain unavailable, posing the most critical challenge  
51 to grassland management, particularly for vulnerable grassland ecosystems in fragile regions grappling  
52 with economic and sustainable development contradictions (Meng et al., 2023; Pozo et al., 2021; Miao et  
53 al., 2020; He et al., 2022). In the early 2000s, the Food and Agriculture Organization of the United  
54 Nations (FAO) launched the Gridded Livestock of the World (GLW) project to facilitate a detailed  
55 evaluation of livestock production, aiming to provide pixel-scale livestock densities instead of traditional  
56 administrative unit benchmarks (Nicolas et al., 2016). Consequently, the world's inaugural dataset of  
57 livestock spatialization map (GLW1) was released in 2007, providing the first globally standardized  
58 livestock density distribution map at a spatial resolution of 0.05 decimal degrees ( $\approx 5$  km at the equator)  
59 for 2002. It was not until 2014 that an updated GLW2 map with a 1 km resolution for 2006 was  
60 released, by using a stratified regression approach, superior spatial resolution predictor variables, and  
61 more detailed livestock census data (Robinson et al., 2014). Furthermore, an evolutionary step in  
62 machine learning technology saw Gilbert et al. (2018) using random forests algorithm to forge a global  
63 livestock distribution map with a 10-km resolution for 2010 (GLW3), succeeding traditional multivariate  
64 regression methods and surpassing the precision of previous GLW1 and GLW2 maps. Beyond these  
65 global mappings, several maps with different scales have also been published, including intercontinental,  
66 national, state or provincial, and local scale (Neumann et al., 2009; Prosser et al., 2011; Van Boeckel et  
67 al., 2011; Nicolas et al., 2016). However, these maps are fundamentally coarse due to constraints such as  
68 the availability of fine scale and contemporary census data, the grazing spatialization method, as well as  
69 the identification of appropriate indicators, thereby limiting their application to local or regional-scale  
70 studies (Nicolas et al., 2016; Gilbert et al., 2018; Robinson et al., 2014). Hence, there is an emergent  
71 demand for more refined grazing map products (Mulligan et al., 2020; Martinuzzi et al., 2021).

72 An exemplar of this need can be observed in the Qinghai-Tibet Plateau (QTP), the world's most  
73 elevated pastoral region and an important grazing area in China (Zhan et al., 2023). It was possessing  
74 abundant grassland that spans 1.5 million km<sup>2</sup>, accounting for 50.43% of China's total grassland area,  
75 with Yak and Tibetan sheep as primary grazing livestock (Feng et al., 2009; Cai et al., 2014; Zhan et al.,  
76 2023). Over recent decades, the QTP has undergone escalating grassland degradation, leading to many  
77 ecological and socio-economic problems, which calls for an urgent need for detailed livestock  
78 distribution dataset (Li et al., 2022a). Unfortunately, despite researchers' efforts at mapping the QTP's  
79 grazing intensity, current livestock dataset still suffer from coarse spatio-temporal resolution and  
80 modelling accuracy. Apart from the aforementioned global grazing dataset, several other maps also  
81 cover the QTP. For instance, Liu et al. (2021) generated annual 250-m gridded carrying capacity maps  
82 for 2000-2019, by employing multiple linear regressions of livestock numbers, population density, NPP,  
83 and topographic features. Li et al. (2021) used machine learning algorithms to produce gridded livestock  
84 distribution data at 1 km resolution for 2000-2015 in western China at five year interval, based on  
85 county-level livestock census data and 13 factors from land use practice, topography, climate, and  
86 socioeconomic aspects, including grassland coverage, arable land coverage, forest land coverage, desert  
87 coverage, NDVI, elevation, slope, daytime surface temperature, precipitation, distance to river, travel  
88 time to major cities, population density, and GDP (Li et al., 2021). A contribution from Meng et al. (2023)  
89 brought forth annual longer time-series grazing maps by using random forests model, integrating climate,  
90 soil, NDVI, water distance, and settlement density to decompose county-level livestock census data to a  
91 0.083° (≈10 km at the equator) grid for 1982-2015 (Meng et al., 2023). Similarly, Zhan et al. (2023) also  
92 used random forests algorithm to combine eleven influence factors to provide a winter and summer  
93 grazing density map at 500 m resolution for 2020 (Zhan et al., 2023).

94 However, although these maps have provided good help in understanding grazing conditions on the  
95 QTP, there are currently still no maps that can satisfy the need for fine-scale grassland management  
96 with a long time span. In addition, the available livestock distribution maps of the QTP still need  
97 improvement in terms of modelling techniques and factor selection to obtain high-precision livestock  
98 spatialization data. For example, traditional methods like multiple linear regression, while proven  
99 fundamental and widely applicable for livestock spatialization (Robinson et al., 2014; Ma et al., 2022),  
100 are being challenged by the development of computational science in recent years. Among them,  
101 machine learning technology is providing new opportunities towards more accurate predictions of  
102 livestock distribution (García et al., 2020). Random forests regression, for instance, is currently widely  
103 used to construct global, national as well as regional livestock spatialization dataset, and has been proved  
104 to have much better accuracy than traditional mapping techniques (Rokach, 2016; Nicolas et al., 2016;  
105 Gilbert et al., 2018; Dara et al., 2020; Chen et al., 2019; Li et al., 2021). Nevertheless, other more  
106 advanced machine learning methods with superior feature learning and more robust generalization  
107 capabilities, remains largely untapped for modelling geographic data (Ahmad et al., 2018; Heddam et al.,  
108 2020; Long et al., 2022). Thus, exploring the potential application of new advanced machine learning  
109 technologies in livestock spatialization remains a critical task. Furthermore, selecting the suitable factors  
110 that influencing livestock grazing preferences is also the other critical challenge for enhancing the  
111 precision of grazing distribution dataset (Meng et al., 2023). Livestock grazing activities are often  
112 affected by abiotic and biotic resources, including climatic and environmental factors (Waha et al.,  
113 2018), herd foraging and grazing behaviours (Garrett et al., 2018; Miao et al., 2020), and  
114 conservation-oriented policies (Li et al., 2021). For instance, regions exceeding elevations of 5,600 m or  
115 slope greater than 40% are customarily unsuitable for grazing (Luo et al., 2013; Mack et al., 2013;

116 Robinson et al., 2014; Chen et al., 2019). Moreover, the livestock generally prefer areas abundant in  
117 water and pasture resources for foraging (Li et al., 2021). Besides, ecological conservation policies also  
118 exert substantial influence, significantly affecting grazing distribution relative to the level of  
119 conservation priority. In addition, the health status of the grassland is an important factor influencing  
120 whether livestock choose to feed or not (Li et al., 2021). Consequently, indicators related to the above  
121 aspects are often employed to gauge the spatial heterogeneity of livestock distribution (Allred et al., 2013;  
122 Sun et al., 2021; Meng et al., 2023). Nonetheless, some most commonly used indicators like NPP or  
123 NDVI can result in misconceptions, as they may not fully characterize the grazing intensity. For example,  
124 grasslands with high NPP or NDVI are often preferred by livestock, but this doesn't necessarily correlate  
125 with grazing intensity in nature reserves due to strict policy restrictions (Veldhuis et al., 2019; O'Neill and  
126 Abson, 2009; Zhang et al., 2021b). Conversely, areas with sparse grassland cover may support  
127 considerable livestock numbers, despite evidence of degradation (Zhang et al., 2021a; Guo et al., 2015).  
128 Accordingly, further investigation of novel indicators is imperative to enhance the correlation between  
129 grassland and grazing intensity, thereby optimizing the integration of such influencing factors into  
130 grazing spatialization models.

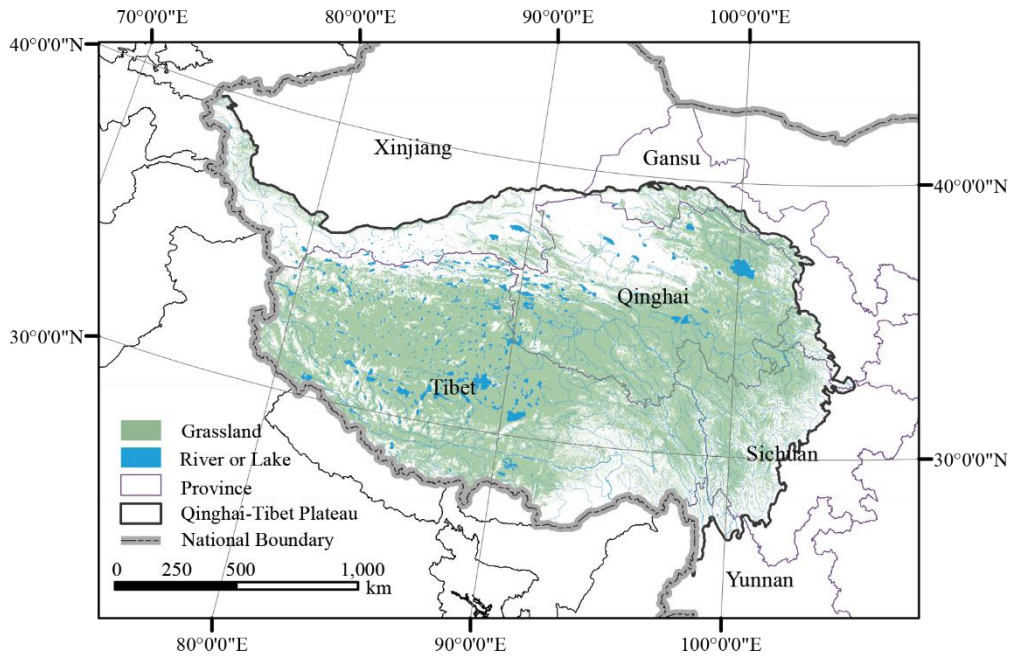
131 In summary, the QTP is in pressing need for a high spatio-temporal resolution grazing dataset to  
132 address urgent and realistic challenges. But the existing livestock dataset specific to the QTP are fraught  
133 with several insufficient, predominantly concerning rough resolution, relatively backward census data,  
134 as well as conventional methods in livestock spatialization. Moreover, the discrepancies in predictive  
135 indicators and modelling approaches within these dataset discourage their application in time-series  
136 analysis. Consequently, the generation of high-resolution and high-quality grazing map products has  
137 emerged as the most pressing challenge for the QTP. Here, we aim to (1) establish a methodological  
138 framework by using more rational models and indicators than traditional studies to achieve fine-scale  
139 livestock spatialization; (2) select the grazing spatialization model with good performance by  
140 incorporating multi-source data with advanced machine learning techniques; and (3) ultimately, provide  
141 an annual grazing intensity dataset with 100 m resolution spanning from 1990-2020. These maps can not  
142 only provide fundamental dataset with finer spatio-temporal resolution to address the limitations of  
143 existing grazing intensity maps, but enhance a better understanding of sustainable management practices  
144 as well as other grassland-related issues across the QTP.

## 145 **2 Data and methods**

### 146 **2.1 Study area**

147 Known as the Asia's water tower and the world's third pole, the QTP is geographically situated  
148 between 73°19'~104°47' east longitude and 26°00'~39°47' north latitude, with a total area of about 2.61  
149 million square kilometers (Figure 1). Its jurisdiction encompasses 182 counties within six provincial  
150 regions of China, including Tibet Autonomous Region, Qinghai Province, Xinjiang Uygur Autonomous  
151 Region, Gansu Province, Sichuan Province, and Yunnan Province (Meng et al., 2023). Elevation on the  
152 QTP predominantly ranges between 3,000 m and 5,000 m, with an average altitude exceeding 4,000 m.  
153 With grasslands constituting over half of its land cover, the QTP emerges as one of the most important  
154 pastoral areas in China. Alpine steppe, alpine meadow, and temperate steppe characterize the main  
155 grassland types on the QTP (Han et al., 2019; Zhai et al., 2022; Zhu et al., 2023b). The complex  
156 geographical and climatic conditions of the QTP contributes to the markedly heterogeneous grassland  
157 distribution, which correspondingly lead to the high heterogeneity in livestock distribution. Moreover,

158 social and economic development, coupled with policy initiatives directed towards grassland restoration,  
159 have noticeably impacted the livestock numbers on the QTP over recent decades (Li et al., 2021; Li et al.,  
160 2016).



161 Figure 1. The geographic zoning map of the Qinghai-Tibet Plateau (QTP) superposed with grassland vegetation.  
162 Boundaries for the six provinces used for statistical analysis are also shown.

## 163 2.2 Data source

### 164 2.2.1 Census livestock data

165 The county-level census livestock data for the period between 1990 and 2020 were obtained from  
166 the Bureau of Statistics of each county across the QTP (Table 1). The data includes the number of cattle,  
167 sheep, horse and mule, with the exception of counties in Yunnan Province, which lack data for the  
168 years from 1990 to 2007, and Ganzi Prefecture in Sichuan Province, which lack data for the years from  
169 1990 to 1999, and Muli county in Sichuan Province, which lack data for the years from 1990 to 2007.  
170 For these counties belonging to the same prefecture, including counties in Ganzi and Aba prefectures in  
171 Sichuan Province, we used the livestock census data at the prefecture-level to carry out spatialization.  
172 For these counties in Yunnan Province, since they belong to different municipalities, it is not reasonable  
173 to replace them with municipal-level data. For these counties without livestock census data for some  
174 years, we supplemented the missing data by linear interpolation with grazing density data in available  
175 year. In total, livestock data were available for 182 counties, and 4,998 independent records were  
176 finally generated. Furthermore, the respective quantities of different livestock types are converted to  
177 Standard Sheep Units (SU), in compliance with the Chinese national regulations (Meng et al., 2023).

178 Due to the difficulty of collecting township-level census livestock data, the validation data at the  
179 township scale collected in this study only involved these townships of Baching County (2010-2018)  
180 and Gaize County (2018-2020) in Tibet, and Hongyuan County in Sichuan Province (2008). The  
181 township-level census livestock data cumulatively involves 18 townships with a total of 112 records,  
182 and were only used for auxiliary validation of the simulation results.

183 The validation data at the pixel scale also encompass a total of 112 records from 68 sites, which

184 were collected from literatures, questionnaires and field surveys. Specifically, 93 records at 49 sites  
 185 spanning the 1990-2021 period were obtained from 17 literatures, 19 records at 19 sites were obtained  
 186 from the questionnaires and the field survey in 2021. The detailed information for these records can be  
 187 found in the Supplementary files (Figure S3 and Table S3).

188 Table 1. Summary of the livestock data used in this study

Variables	Scale	Time	Sources
Livestock numbers	County	1990-2020	Statistical bureau
	Township	2008-2020	Statistical bureau
	Pixel	1990-2021	Literatures, questionnaires and field surveys

189 *2.2.2 Factors affecting grazing activities*

190 Livestock grazing activities are often affected by abiotic and biotic resources, including climatic  
 191 and environmental factors (Waha et al., 2018), herd foraging and grazing behaviours (Garrett et al.,  
 192 2018; Miao et al., 2020). For instance, high-altitude and steep hillsides are unsuitable for grazing due to  
 193 terrain constraints, and the distribution of herders directly affects the grazing areas (Luo et al., 2013;  
 194 Mack et al., 2013; Robinson et al., 2014; Chen et al., 2019). Moreover, the livestock generally prefer  
 195 areas abundant in water and pasture resources for foraging (Li et al., 2021). Therefore, in this study,  
 196 topography, climatic, environmental and socio-economic impacts were considered as influential factors  
 197 on grazing activities (Li et al., 2021; Meng et al., 2023).

198 We utilized correlation analysis and the Random Forest importance ranking tool to eliminate  
 199 redundant environmental factors and determine the contribution of each factor. Ultimately, altitude,  
 200 slope, distance to water source, population density, air temperature, precipitation and human-induced  
 201 impacts on NPP (HNPP) was selected as indicators (Table 2). Specifically, elevation is derived from the  
 202 DEM dataset accessible via the Resource and Environmental Data Cloud Platform of the Chinese  
 203 Academy of Sciences (<https://www.gscloud.cn>), which also facilitated slope calculation. Rivers and  
 204 lakes were obtained from the National Tibetan Plateau Data Center (<https://data.tpdac.ac.cn>), and the  
 205 nearest Euclidean distance from each pixel to rivers or lakes is calculated accordingly. Meteorological  
 206 elements such as daily air temperature and precipitation were downloaded from the China  
 207 Meteorological Data Service Center (<http://data.cma.cn>). For the grid dataset that is not conditionally  
 208 available, including population density, temperature, precipitation and HNPP, we detailed the creation  
 209 process in the Supplementary file. All datasets utilized in this study were harmonized to consistent  
 210 coordinate systems and resolutions (WGS 1984 Albers, 100 m).

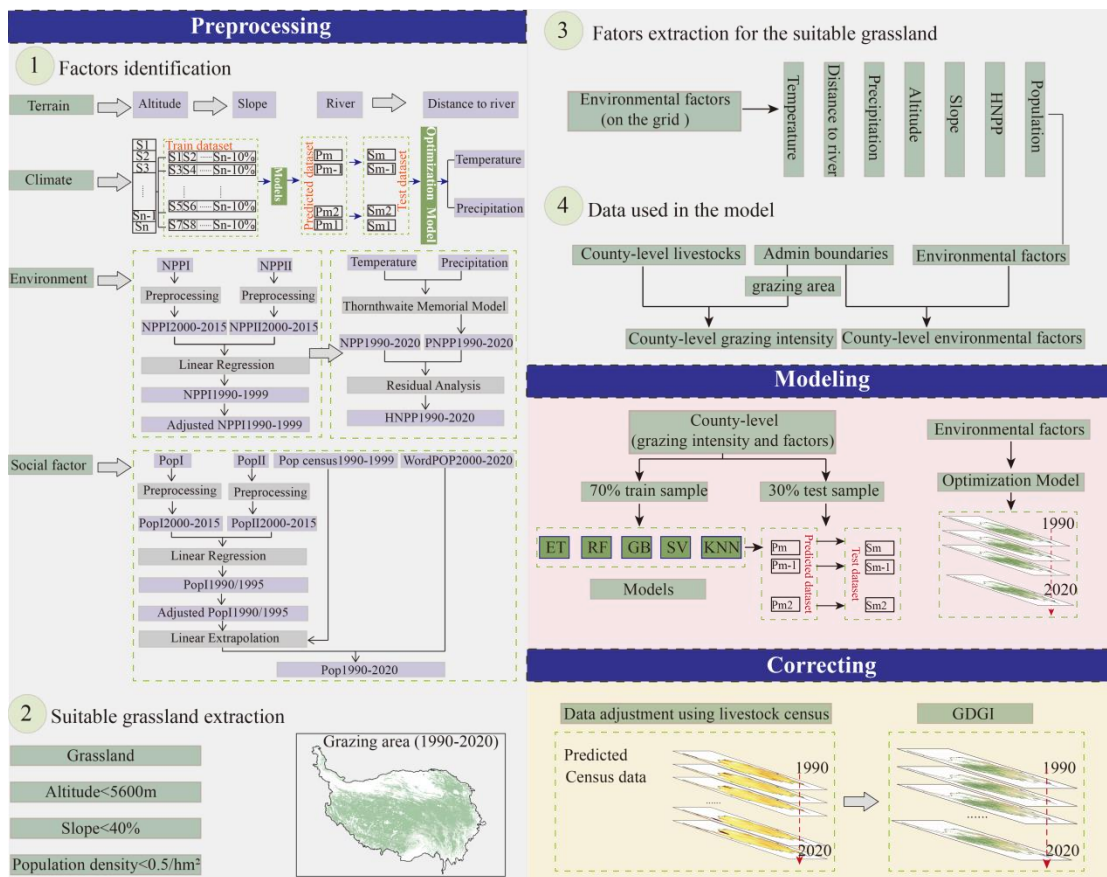
211 Table 2. Summary of factors affecting grazing activities on the QTP.

Variables	Format	Period	Time Resolution	Spatial Resolution	Source
Altitude	GeoTIFF	---	---	30m	<a href="https://www.gscloud.cn">https://www.gscloud.cn</a>
Slope	GeoTIFF	---	---	30m	<a href="https://data.tpdac.ac.cn">https://data.tpdac.ac.cn</a>
Water source	Shapefile	1990-2020	Annual	---	<a href="https://data.tpdac.ac.cn">https://data.tpdac.ac.cn</a>
Population density	GeoTIFF	1990-2020	Annual	100m	See supplementary file

Temperature	GeoTIFF	1990-2020	Annual	100m	See supplementary file
Precipitation	GeoTIFF	1990-2020	Annual	100m	See supplementary file
HNPP	GeoTIFF	1990-2020	Annual	100m	See supplementary file

212 **2.3 Methodological framework**

213 We adopted a comprehensive methodological framework for mapping high-resolution grazing  
 214 intensity on the QTP. This study applied FAO’s assumption that the relationship between environmental  
 215 factors and livestock intensity is identical at both the administrative and pixel level. Three major steps  
 216 are included to predict the distribution pattern of grazing intensity: (1) identifying factors affecting  
 217 grazing activities and extracting theoretical suitable areas for livestock grazing, (2) building grazing  
 218 spatialization model, and (3) filtering the model and correcting the grazing map. An exhaustive  
 219 explanation of each step is provided in Figure 2.



220  
 221 Figure 2. Flowchart of creating grazing intensity maps using different methods and source products.

222 **2.3.1 Identifying factors and theoretical suitable areas for grazing**

223 In this study, we assumed that grazing activities are confined solely to grassland. Consequently, the  
 224 potential grazing areas for each year were identified on the basis of grassland boundaries, which was  
 225 extracted from the 30 m annual land cover dataset (CLCD) (Yang and Huang, 2021). Furthermore,  
 226 grassland with slope over 40% and elevation higher than 5,600 m respectively, were considered  
 227 unsuitable for grazing and were therefore excluded from the potential grazing area in the subsequent

228 simulations (Robinson et al., 2014). In addition, the grassland with population density greater than 50  
229 inhabitants km<sup>-2</sup> were also excluded (Li et al., 2018). The remaining isolated grassland was thus  
230 categorized as theoretical feasible grazing regions.

231 The spatial patterns of abiotic and biotic resources, incorporating food availability, environmental  
232 stress, and herder preference critically affect grazing activities (Meng et al., 2023). In light of this,  
233 seven influencing factors in four aspects were selected for grazing intensity mapping (Figure 2-1).

### 234 2.3.2 Building grazing spatialization model

235 By performing regional statistics, the annual average values for each grazing influence factor were  
236 extracted from the theoretically suitable grazing areas at the county scale, and were further used as  
237 independent variables in the model construction. The dependent variable for the model was acquired by  
238 determining the livestock density within each county, followed by a logarithmic transformation of the  
239 values to normalize the distribution of the dependent variable. Consequently, a total of 4,998 samples  
240 were derived from the aforementioned independent and dependent variables. Of these samples, 70%  
241 were allocated for model training, while the remaining 30% comprised the test sets, serving to validate  
242 the model's performance. Subsequently, we built grazing spatialization models using five machine  
243 learning algorithms at the county scale, including Support Vector regression (SV) (Cortes and Vapnik,  
244 1995; Lin et al., 2022), K-Nearest Neighbors (KNN) (Cover and Hart, 1967), Gradient Boosting  
245 regression (GB) (Friedman, 2001; Pan et al., 2019), Random Forests (RF) (Breiman, 2001) and Extra  
246 Trees regression (ET) (Geurts et al., 2006; Ahmad et al., 2018) (see Supplementary file for details).  
247 Lastly, to assess the accuracy of the spatialized livestock map, the predicted livestock intensity values  
248 were juxtaposed with the livestock statistical data from each respective county.

### 249 2.3.3 Correcting the grazing map

250 We further used the optimal model to predict the geographical distribution of grazing density across  
251 the QTP. To maintain better consistency between the predicted livestock number and the census data,  
252 the estimated results were adjusted using the census livestock numbers at the county scale as a control  
253 according to Equation (1). Consequently, the corrected and refined map is presented as the final grazing  
254 intensity map in this study.

$$255 \quad L_{correction} = \frac{L_{CCensus}}{L_{Cgrid}} \times L_{grid} \quad (1)$$

256 where  $L_{correction}$  is the predicted pixel-scale livestock number after adjustment,  $L_{Cgrid}$  represents the  
257 estimated livestock number for each county,  $L_{CCensus}$  is the census livestock number for each county,  
258 and  $L_{grid}$  refers to the predicted livestock number at the pixel scale.

## 259 2.4 Accuracy evaluation

260 We used three accuracy validation indexes to evaluate the performance of five machine learning  
261 algorithms, including coefficients of determination ( $R^2$ ), mean absolute error (MAE), and root mean  
262 square error (RMSE), by through a comparison of the predicted value with the census data. The  
263 definitions of three metrics are presented in Equation (2) to (4).

$$264 \quad R^2 = 1 - \frac{\sum_{i=1}^n (C_i - P_i)^2}{\sum_{i=1}^n (C_i - \bar{C})^2} \quad (2)$$



265 
$$\text{MAE} = \frac{1}{n} \sum_{i=1}^n |C_i - P_i| \quad (3)$$

266 
$$\text{RMSE} = \sqrt{\frac{1}{n} \sum_{i=1}^n (C_i - P_i)^2} \quad (4)$$

267 where  $C_i$  and  $P_i$  are the census livestock data and the predicted value for county  $i$ , respectively;  $\bar{C}$   
 268 represents the mean census value for all county; and  $n$  gives the total number of counties.

269 **2.5 uncertainties evaluation**

270 Uncertainty in our grazing intensity maps can stem from multiple sources, such as the constraints of  
 271 cross-scale modeling and the intrinsic inaccuracies of the input data. To quantify these uncertainties, we  
 272 utilized the Monte Carlo (MC) method, conducting 100 iterations of simulation. Subsequently, we  
 273 evaluated uncertainty through the Mean Relative Error (MRE) and assessed the model's robustness  
 274 using the Standard Deviation (STD), following established methodologies (Yang et al., 2020;  
 275 Alexander et al., 2017; Mcmillan et al., 2018). The definitions for these metrics are delineated in  
 276 Equations (5) to (7).

277 
$$\text{MC} = \frac{1}{n} \sum_{i=1}^n f(x_i) \quad (5)$$

278 
$$\text{MRE} = \frac{1}{n} \sum_{i=1}^n \left| \frac{x_i - \bar{x}}{\bar{x}} \right| \quad (6)$$

279 
$$\text{STD} = \frac{1}{n} \sum_{i=1}^n f(x_i) \sqrt{\frac{1}{n} \sum_i^n (x_i - \bar{x})^2} \quad (7)$$

280 where  $x_i$  are random samples,  $f(x_i)$  is the function evaluated at  $x_i$ , and  $n$  is the number of  
 281 simulations.  $\bar{x}$  represents the mean value for all simulation maps.

282 **3 Results**

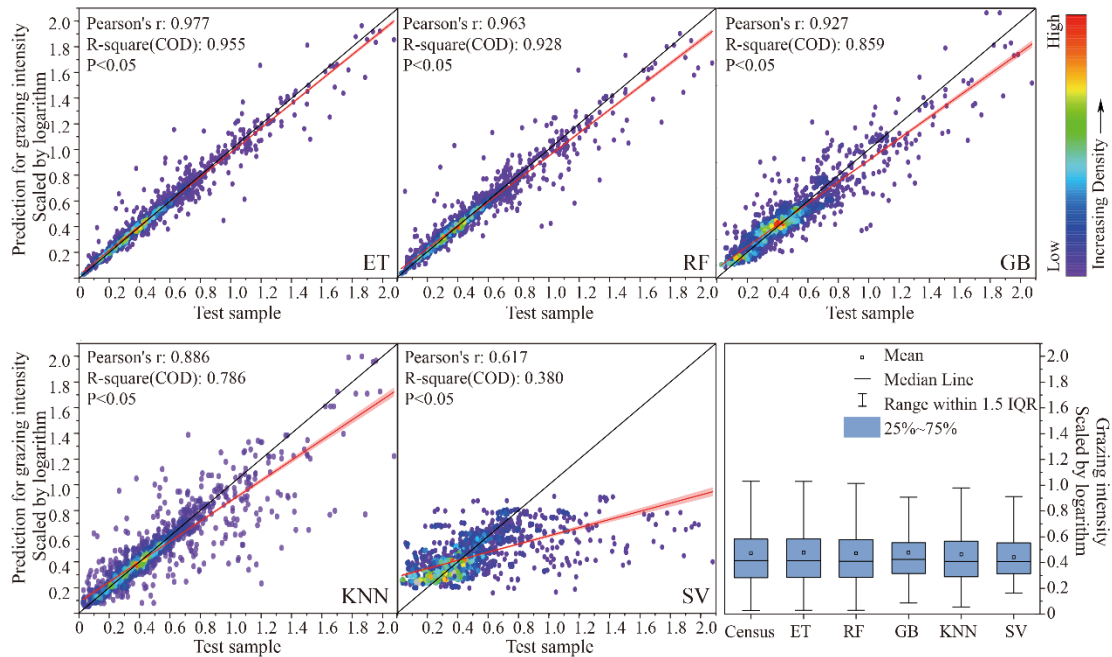
283 **3.1 Performances of models**

284 Table 3 summarizes the efficiency of the five used machine learning models with considering all  
 285 three accuracy evaluators of  $R^2$ , MAE and RMSE. It can be seen that the ET model performs the best,  
 286 with its  $R^2$  exceeding 0.955, and MAE (0.081 SU/hm<sup>2</sup>) and RMSE (0.164 SU/hm<sup>2</sup>) significantly lower  
 287 than the value of RF, GB, KNN and SVM models. Figure 3 illustrates the correlation between the  
 288 census livestock data and the livestock numbers predicted by the model for each county from 1990 to  
 289 2020. It demonstrated that the ET-predicted data displayed a distribution pattern consistent with that of  
 290 other models, but the scatter points of the ET model were more convergent to the 1:1 diagonal line,  
 291 indicating a superior fit compared to the other models. These comparisons suggest that the ET model  
 292 possesses superior robustness and can, therefore, provide stable estimations of livestock intensity on  
 293 the QTP.

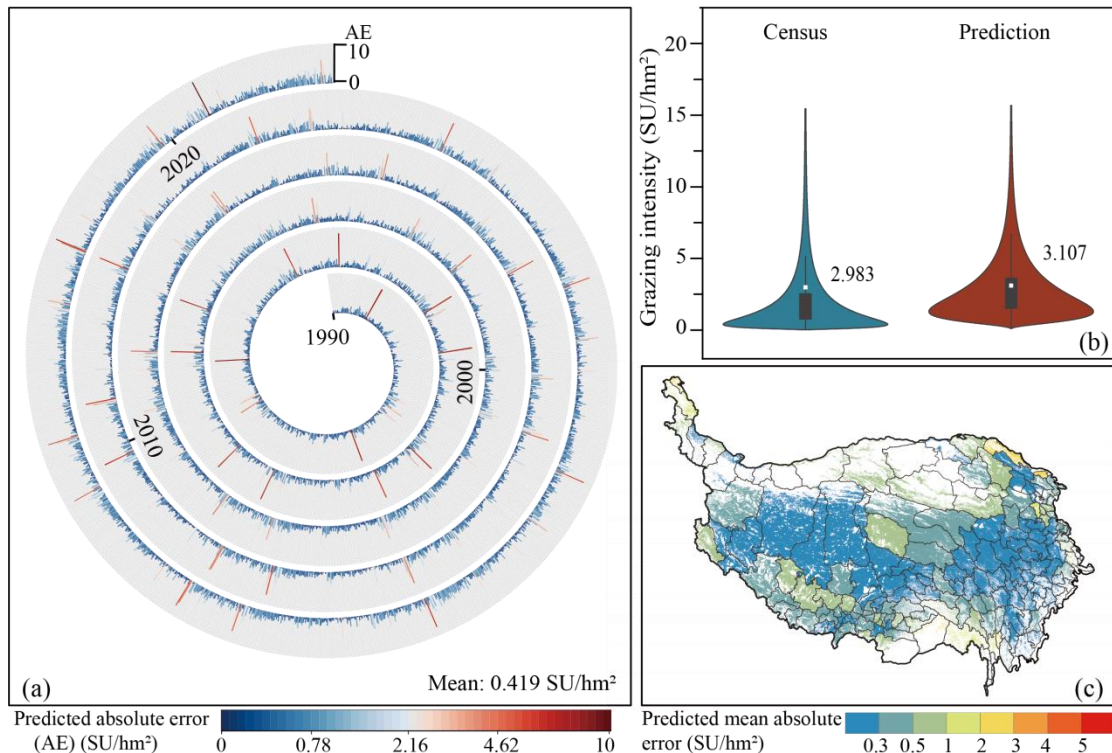
294 Table 3. Comparison of mapping accuracy for five machine learning models based on the same validation datasets

Models	$R^2$	MAE (SU/hm <sup>2</sup> )	RMSE (SU/hm <sup>2</sup> )
ET	0.955	0.081	0.164
RF	0.928	0.099	0.208
GB	0.859	0.197	0.300
KNN	0.786	0.186	0.384
SVM	0.380	0.419	0.750

295 *Note:* The MAE and RMSE have calculated using inverse logarithmic transformation, presenting the  
 296 actual values.



297  
 298 Figure 3. Scatterplots of model-predicted livestock numbers and census grazing data (scaled by logarithm) at the  
 299 county level. The red solid line and the black solid line are the fitting line and the 1:1 diagonal line, respectively.



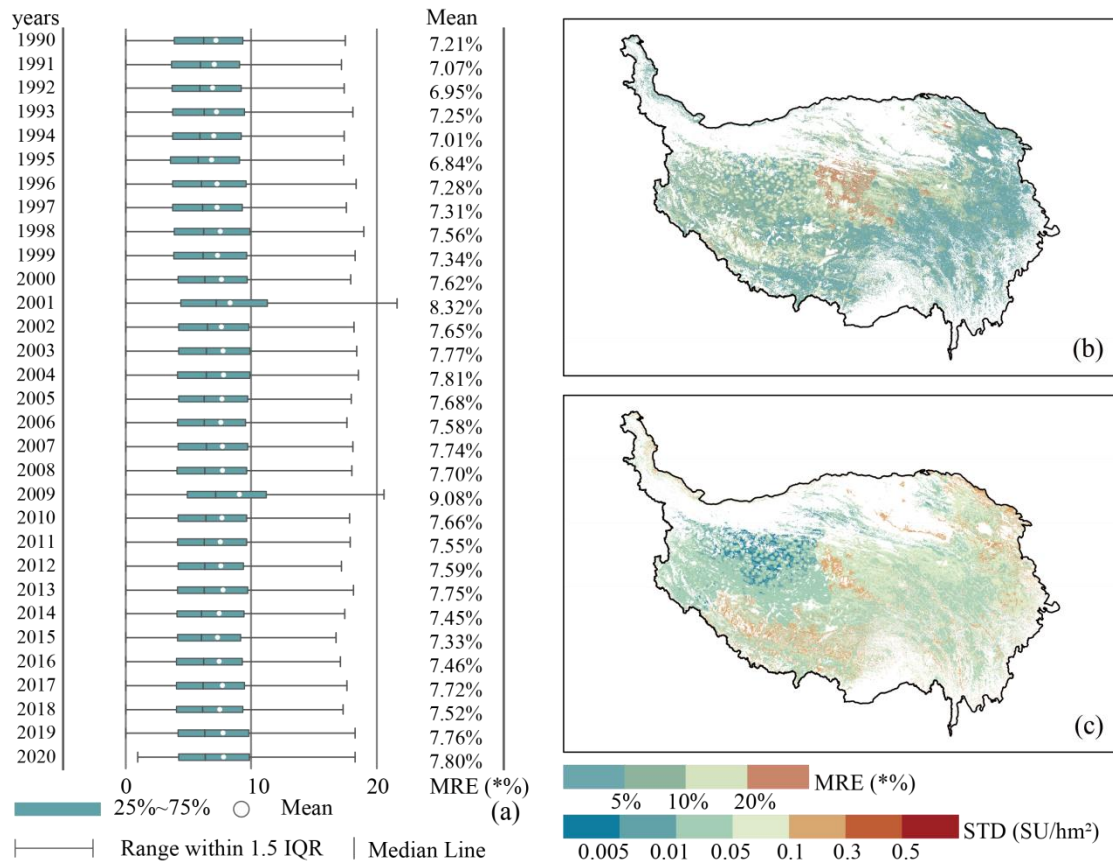
300  
 301 Figure 4. Accuracy of the ET-predicted grazing intensity results at spatial resolution of 100 m from 1990 to 2020.  
 302 (a) absolute error (AE) between the predicted and the census data at the county scale from 1990 to 2020; (b)  
 303 comparison of the predicted and census data of the whole QTP from 1990 to 2020; (c) spatial distribution of the  
 304 mean absolute error (MAE) during 1990 to 2020 for each county.

305 Using the ET model, we projected the spatio-temporal distribution of grazing intensity across the

306 QTP from 1990 to 2020 at a 100 m × 100 m resolution. To validate the accuracy of these predictive  
307 maps, we up scaled the pixel-level predictions to the county level and compared them against livestock  
308 census data (Figures 4a and 4b). The results clearly show a high degree of consistency between the  
309 predicted livestock intensity and the county-level census data, especially in areas with lower grazing  
310 intensity (Figures 4a and 4b). Specifically, while the mean census data indicated 2.983 SU/hm<sup>2</sup> for  
311 livestock intensity, our county-level predictions yielded an average of 3.106 SU/hm<sup>2</sup>, with a MAE of  
312 0.123 SU/hm<sup>2</sup>, a RMSE of 0.580 SU/hm<sup>2</sup>, and an R<sup>2</sup> value of 0.669. Additionally, 76.31% of the  
313 counties (n = 3,814) exhibited data discrepancies of no more than 0.6 SU/hm<sup>2</sup>, and 91.74% (n = 4,585)  
314 had discrepancies under 1.0 SU/hm<sup>2</sup>. Regarding spatial distribution, areas with data discrepancies of  
315 less than 0.3 SU/hm<sup>2</sup> were predominantly located in the northwest and southeast regions of the QTP. In  
316 certain counties of the northeast and southwest, the variations were even below 1.0 SU/hm<sup>2</sup> (Figure 4c).

### 317 **3.2 Evaluation of uncertainties**

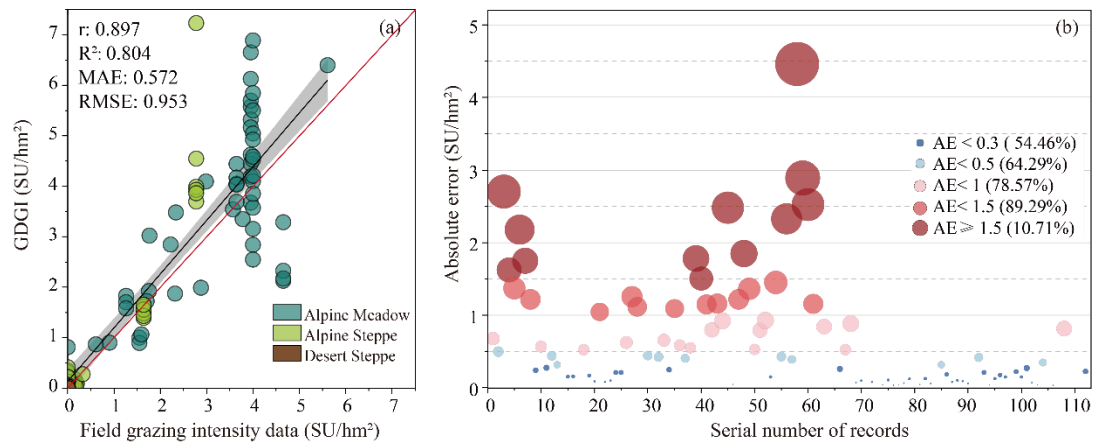
318 We have chosen the Mean Relative Error (MRE) as a key metric for evaluating the simulation  
319 accuracy of grazing intensity within the QTP. Employing Monte Carlo simulations spanning the period  
320 from 1990 to 2020, our research findings demonstrate that the average MRE for grazing intensity  
321 across the QTP ranged between 6.84% and 9.08% (Figure 5a). The spatial distribution of MRE  
322 indicates that the majority of the plateau exhibits low error margins. For example, in 2020, areas with  
323 an MRE of less than 5% accounted for 35.86% of the total grassland area, while those with an MRE  
324 below 10% constituted 75.84%. Only 3.38% of the grasslands had an MRE exceeding 20%, with these  
325 regions primarily located in the southwestern portion of the QTP (Figure 5b). Moreover, the robustness  
326 analysis suggests that the majority of regions within the QTP display relatively stable grazing intensity  
327 trends. For instance, the overall standard deviation (STD) in 2020 was 0.059 SU/hm<sup>2</sup>, with the  
328 northwest region demonstrating remarkable stability, reflected in an STD of less than 0.005 SU/hm<sup>2</sup>.  
329 Although some areas within the Yarlung Zangbo River Basin and the eastern part of Qinghai Province  
330 experienced higher variability, their STD was still maintained below 0.3 SU/hm<sup>2</sup> (Figure 5c).



331  
 332 Figure 5. Uncertainty analysis of grazing intensity maps based on ET and Monte Carlo methods. (a) MRE of  
 333 grazing intensity maps from 1990 to 2020, (b) spatial distribution of MRE, (c) spatial distribution of STD.

334 **3.3 Validation of the GDGI dataset**

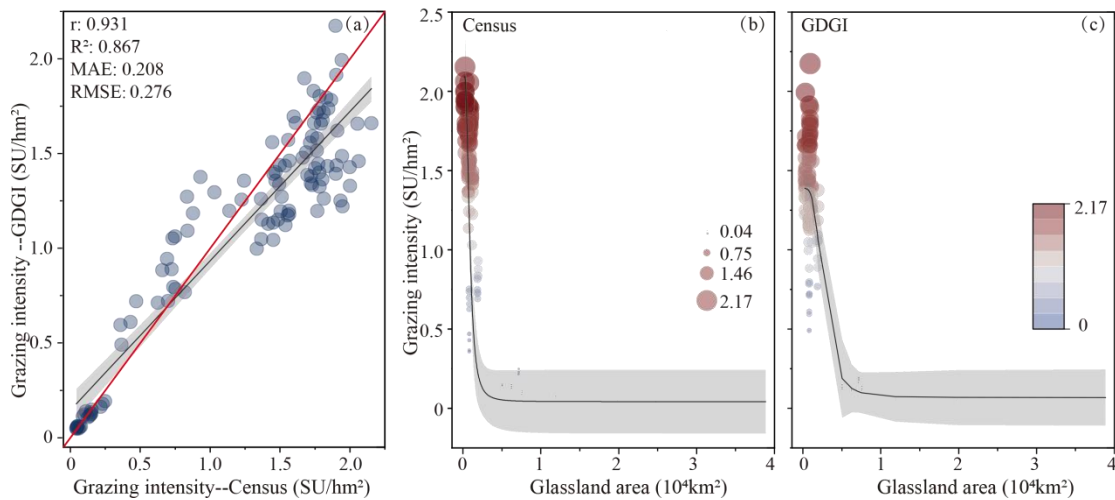
335 After employing county-level livestock census as a benchmark for quality control, we obtained the  
 336 annual Gridded Dataset of Grazing Intensity maps (GDGI) across the QTP spanning 31 years from  
 337 1990 to 2020. We firstly confirmed the accuracy of the GDGI dataset based on 112 field grazing  
 338 intensity records at 68 sites (see Table S3 in Supplementary file for details), which ranged from 0 to  
 339 5.61 sheep unit per hectare (SU/hm<sup>2</sup>), and covered three main grasslands on the QTP: the alpine steppe  
 340 (N = 62), alpine meadow (N = 46), and alpine desert steppe (N = 4). The GDGI dataset was assessed by  
 341 undertaking a comparative accuracy assessment between it and the field grazing intensity data (Figure  
 342 6a). It can be seen that in general, our dataset was highly consistent with the reference ground-truth  
 343 validation data, with  $R^2 = 0.804$ ,  $MAE = 0.572$  SU/hm<sup>2</sup>, and  $RMSE = 0.953$  SU/hm<sup>2</sup>. Moreover, the  
 344 absolute errors between the GDGI data and the field grazing intensity data were relatively small, with  
 345 more than half of the records having an error below 0.3 SU/hm<sup>2</sup>, 78.57% below 1.0 SU/hm<sup>2</sup> and 89.29%  
 346 below 1.5 SU/hm<sup>2</sup> (Figure 6b).



347

348 Figure 6. Validation of the GDGI dataset using 112 field grazing intensity records at the pixel scale: (a) linear  
 349 fitting results; (b) absolute error (AE) distribution.

350 We further validated the precision of the GDGI dataset using the township-level livestock census  
 351 data. Encouragingly, the evaluation results showed that the GDGI dataset has excellent performance at  
 352 the township scale (Figure 7a), with  $R^2$  of 0.867, MAE of 0.208  $\text{SU}/\text{hm}^2$ , and RMSE of 0.276  $\text{SU}/\text{hm}^2$ .  
 353 In addition, similarly to the census data, the GDGI dataset indicated that some townships with few  
 354 grasslands area are still under high grazing pressure (Figure 7b and 7c).



355

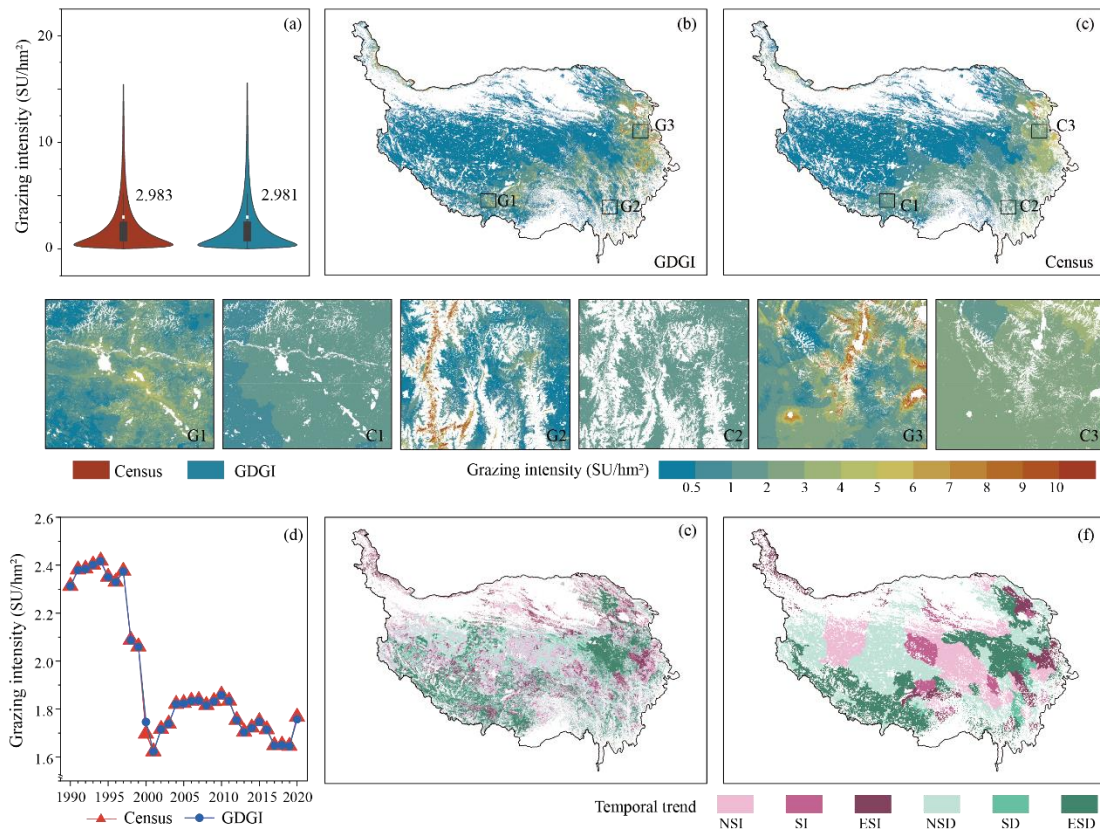
356 Figure 7. Validation of the GDGI dataset using census livestock data at the township level: (a) linear fit of  
 357 predicted number and census data; (b-c) logistic fit of grazing intensity data and grassland area.

### 358 3.4 Spatio-temporal variations of grazing intensity

359 In terms of the temporal trends of grazing intensity, the GDGI dataset overall exhibited consistent  
 360 trends with the livestock census data (Figure 8d-8f). Specifically, the census data indicated the  
 361 livestock numbers remained high and largely stable from 1990 to 1997, followed by a sharp decline  
 362 from 1997 to 2001, and then remained a period of fluctuation post-2001, which was successfully  
 363 captured by the GDGI dataset. Moreover, the spatial heterogeneity of grazing intensity within the  
 364 counties over the QTP was also effectively reflected by the GDGI dataset, a characteristic not  
 365 illustrated by the census dataset. For example, areas of high grazing intensity were concentrated in the

366 northeastern and south-central regions of the plateau, mainly including the eastern part of Qinghai  
 367 Province, the southwestern part of Gansu Province, the northwestern part of Sichuan Province, and the  
 368 eastern region of the Tibet Autonomous Region (Figure 8e and 8f).

369 Over the past 31 years, 63.95% of the plateau's grassland showed a decreasing trend in grazing  
 370 intensity, with 49.80% showing significant decreases, primarily located in the eastern Sanjiangyuan  
 371 area and the southwestern region of the QTP (Figure 8e and 8f). Meanwhile, grazing intensity was  
 372 increasing in 36.05% of the grassland, but most of them (60.16%) did not reach the level of  
 373 significance and were mainly distributed in the northeastern plateau (Figure 8e and 8f).



374  
 375 Figure 8. Validation of the GDGI maps using the census grazing data from 1990 to 2020: (a) violin plot of the  
 376 census data and the predicted value; (b-c) spatial distribution in SU per pixel; (d) temporal change in SU per year  
 377 (only including 124 counties with livestock census data); (d-f) spatial distribution of SU changes tested by sen's  
 378 slope and Mann-Kendall. Note: ESI for Extremely Significant Increase (slope>0 &  $p<0.01$ ); SI for Significant  
 379 Increase (slope > 0 &  $p < 0.05$ ); NSI for Non-significant increase (slope>0 &  $p>0.05$ ); ESD for Extremely  
 380 Significant Decrease (slope<0 &  $p<0.01$ ); SD for Significant decrease (slope<0 &  $p<0.05$ ); NSD for  
 381 Non-significant decrease (slope<0 &  $p>0.05$ ).

## 382 4 Discussion

### 383 4.1 Comparison with other grazing intensity maps

384 To further assess the effectiveness and reliability of the developed GDGI dataset, the mapping  
 385 results were juxtaposed with seven publicly available grazing intensity maps covering the QTP (Table  
 386 4). It can be seen that despite their public availability, these maps lacked both in spatial and temporal

387 resolution when juxtaposed with the GDGI maps. Our analysis was extended to four openly accessible  
388 gridded livestock datasets, including GI-Sun (Sun et al., 2021), ALCC (Liu, 2021), GI-Meng (Meng  
389 et al., 2023) and GLWs (Gilbert et al., 2018). A commonality among all five maps was the consistency  
390 for the spatial patterns of grazing intensity, with prevalent high and low intensities in the northeast and  
391 northwest regions, respectively (Figure 9). However, these maps differed significantly in terms of  
392 accuracy. As the grazing intensity maps of GLWs and ALCC were produced based on the livestock  
393 census data in 2001 and 2015, an accuracy comparison for the corresponding years was conducted  
394 among the five datasets both at county and township scale. Observations at the county scale indicate  
395 that all four datasets, with the exception of GI-Sun, are largely in alignment with the county census  
396 data (Figure 9b). When examined at the township scale, GI-Sun and GLW demonstrate the most  
397 significant discrepancies, with MRE surpassing 68%. ALCC and GI-Meng follow, recording MREs of  
398 30.69% and 38.80%, respectively. Additionally, the GDGI shows the highest degree of accuracy in  
399 relation to the township census data, as indicated by the lowest MAE and RMSE values (Figure 9c).  
400 Moreover, the GDGI dataset spanning 31 years (1990-2020) earmarked it as a more suitable choice for  
401 long-term studies in comparison to the other four datasets. Regarding spatial distribution, the overall  
402 patterns of these grazing maps are largely consistent, exhibiting higher density patterns in the southeast  
403 and lower in the northwest. However, notable discrepancies are still apparent in the finer details. In  
404 general, in terms of visually representing the spatial distribution of livestock, the GDGI maps  
405 exhibit the best performance.

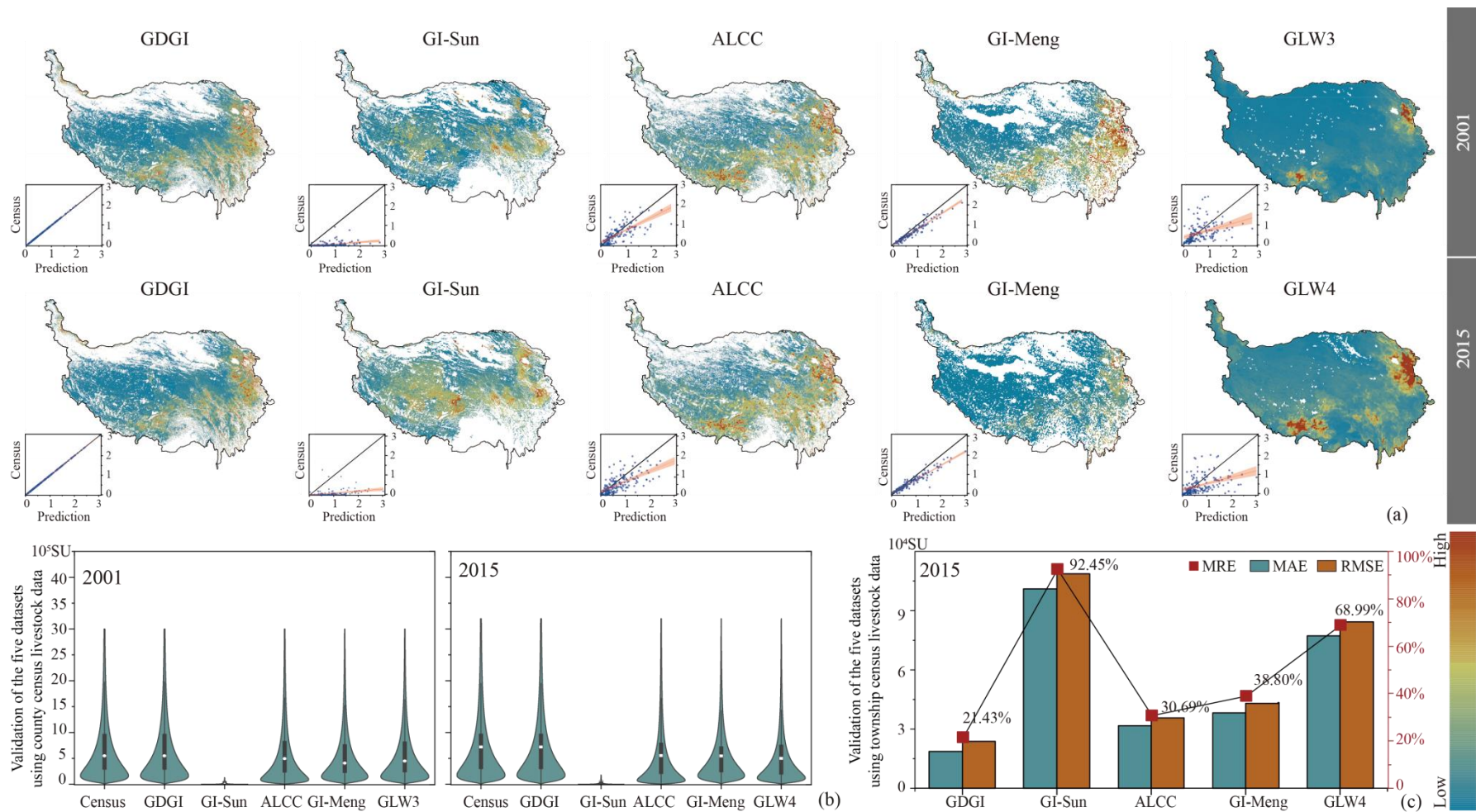
406 Several potential factors may contribute to the improved accuracy of the GDGI. First, the livestock  
407 census data used in GDGI is more detailed, aiding in enhancing the accuracy of the estimation results.  
408 Specifically, GI-sun, ALCC, GI-Meng and GDGI all use county-level livestock statistics to map  
409 grazing intensity, whereas GLW3 and GLW4 are based on provincial-level census data to map, which  
410 results in their accuracy lagging significantly behind the four other datasets (Nicolas et al., 2016; Sun et  
411 al., 2021). Second, grazing densities are estimated by dividing the number of livestock from the  
412 statistical data, after a mask excluding theoretical unsuitable grazing areas. However, these maps differ  
413 in their definitions of suitable grazing areas. In this study, as with the GI-sun and GI-Meng maps, we  
414 considered grazing to occur only on grasslands, and further excluded unsuitable areas such as high  
415 elevations and steep slopes. This kind of definition is clearly more reasonable than the GLW series,  
416 which removed only water bodies, urban core areas, and protected areas with relatively tight  
417 regulations of human activity (Mcsherry and Ritchie, 2013; He et al., 2022). However, the GI-Meng  
418 dataset considers the core areas of protected areas as grazing-free region, it does not match the actual  
419 situation on the QTP (Jiang et al., 2023; Li et al., 2022b; Zhao et al., 2020). Those different thresholds  
420 for the definition of suitable grazing areas are account for the fact each map has different theoretical  
421 grazing regions. Third, the selection of models and environmental factors may also be a significant  
422 contributing factor, leading to variations in predictive accuracy. For instance, different algorithms were  
423 employed, including linear regression and machine learning methods (Nicolas et al., 2016; Li et al.,  
424 2021). Additionally, the environmental factors considered varied; specifically, the GDGI utilized the  
425 Human-induced Net Primary Productivity (HNPP) to represent grasslands, whereas other maps relied  
426 on Net Primary Productivity (NPP) and Normalized Difference Vegetation Index (NDVI) (Allred et al.,  
427 2013; Sun et al., 2021; Meng et al., 2023).

428 Table 4. Summary of map-derived parameters for this study and other seven public gridded livestock datasets covering the QTP.

<b>Dataset</b>	<b>Accessibility</b>	<b>Census</b>	<b>Temporal resolution</b>	<b>Spatial resolution</b>	<b>Period (years)</b>	<b>Method</b>	<b>Livestock type</b>
GDGI	Yes	County	annual	100 m	1990-2020 (31)	ET	Standard SU
GLW3	Yes	Province/sub-Province	annual	0.083°(≈ 10 km)	2001 (1)	RF	Cattle, ducks, pigs, chickens,
GLW4	Yes	Province/sub-Province	annual	0.083°(≈ 10 km)	2015 (1)	RF	sheep, goats
GI-Sun	Yes	County	five-year interval	1 km	1990-2015 (6)	LRA	Standard SU
ALCC	Yes	Province/sub-Province	annual	250 m	2000-2019 (20)	MLR	Standard SU
GI-Meng	Yes	County	annual	0.083°(≈ 10 km)	1982-2015 (34)	RF	Standard SU
GI-Li	No	County	five-year interval	1 km	2000-2015 (4)	DNN	Cattle and sheep
GI-Zhan	No	County	season	15'' (≈ 500 m)	2020 (2)	RF	Standard SU

429 Note: LRA is the abbreviation of linear regression analysis.





430

431 Figure 9. Comparisons of different grazing datasets for the years 2001 and 2015: (a) spatial patterns; (b) predicted livestock number and census data at county scale; (c) accuracy evaluation

432 between predicted livestock number and census data at township scale.

## 433 4.2 Spatial heterogeneity of grazing intensities

434 In general, the multiyear average grazing intensity on the QTP increased from west to east during  
435 1990 to 2020, with broad spatial heterogeneity (Figure 8). Highest grazing intensity was found mainly  
436 in the northeastern and south-central regions of the Plateau (mostly higher than 5.0 SU/hm<sup>2</sup>), while  
437 they were lowest in the northwest (mostly less than 1.0 SU/hm<sup>2</sup>). Over the past 31 years, the average  
438 grazing intensity decreased across most of the Plateau, but 36.05% of the entire QTP grassland still  
439 encountered continuous grazing intensity increase, especially in the northeastern regions (Figure 8).

440 The spatial heterogeneity of grazing intensities on the QTP may be attributed to the following  
441 reasons. First, complex geographic and climatic conditions on the QTP determine the heterogeneity of  
442 grassland, which in turn affects livestock distribution (Wang et al., 2018; Wei et al., 2022). In general,  
443 the grazing intensity patterns shown in the GDGI maps are basically consistent with the stocking rate  
444 threshold patterns in the QTP grasslands, both decreased from east to west (Zhu et al., 2023a). This  
445 phenomenon partially reflects the heterogeneity of the grasslands, as the alpine meadows and the  
446 steppes mainly distributed in the east and the west, respectively. Second, the dynamics of  
447 socio-economic development are obviously another important factors determining grazing intensity. In  
448 areas falling behind in terms of the socio-economic indicators, herders prefer to increase livestock in  
449 efforts to improve household incomes, leading to greater pressure on grasslands in these regions (Fang  
450 and Wu, 2022). In addition, the perceived increases in human population also resulted in the  
451 considerably increased need to more livestock (Wei et al., 2022).

452 The grazing intensity dynamics across the QTP are partly reflective of the impacts of various  
453 management policies that have been implemented over distinct periods. For example, a significant  
454 increase in grazing intensity on the QTP was observed in the early 1990s, potentially a direct result of  
455 the introduction of the household contract responsibility system. Moreover, the grazing intensity  
456 experienced a pronounced decline from 1997 to 2001, as illustrated in Figure 8d, indicative of the  
457 adverse effects of natural disasters. Notably, the severe snowstorms that struck Naqu in the central QTP  
458 during 1997-1998 are documented to have caused the mortality of over 820,000 livestock (Ye et al.,  
459 2020). Figure 8d further delineates a considerable upsurge in grazing intensity on the QTP between  
460 2000 and 2010, aligning with the trends reported by Sun et al. (2021) and Li et al. (2021). This  
461 observed increase may be attributed to a rebound in grazing activity following the aforementioned  
462 natural disasters. In addition, Figure 8d indicates a sustained decrease in grazing intensity post-2010  
463 across the plateau, which can be predominantly ascribed to the implementation of extensive ecological  
464 conservation projects.

## 465 4.3 Implications for grazing management

466 Nearly half of the grasslands on the QTP have been reported to be degraded over the past four  
467 decades (Wang et al., 2018; Dong et al., 2020), with some reports even indicating that the degraded  
468 grassland has reached 90% (Wang et al., 2021). It is widely recognized that overgrazing is the  
469 predominant and most pervasive unsustainable human activity continuing to drive grassland  
470 degradation on the QTP (Wang et al., 2018; Chen et al., 2019). Generally, these degraded grassland on  
471 the QTP can be effectively restored by adaptive management (Wang et al., 2022). However, better  
472 management of grasslands requires a deeper understanding of the anthropogenic activities, which still  
473 remain an important challenge and can be effectively addressed by the GDGI dataset.

474 According to the GDGI maps generated in this study, high-intensity grazing activities are mainly  
475 concentrated in the northeastern as well as the south-central part of the QTP, with the grazing intensity  
476 in some areas even nearly more than ten times than the average value of the entire plateau (Figure 6b),  
477 and have exceeded the stocking rate threshold of these grasslands (Zhu et al., 2023a). Population  
478 growth and the related increasing livelihood demands is one of the main reasons for this increase. To  
479 meet daily needs and enhance household income, the herders have endeavored to increase livestock,  
480 thereby intensifying grazing pressures on the grasslands over the QTP (Fang and Wu, 2022; Abu  
481 Hammad and Tumeizi, 2012). Although the current average grazing intensity in the northwest QTP  
482 (around 1.0 SU/hm<sup>2</sup>) is below their average stocking rate threshold (around 1.5 SU/hm<sup>2</sup>) (Zhu et al.,  
483 2023a), the grassland management should still be given adequate attention. Because as the most arid  
484 areas with low stocking rate threshold on the QTP, the grazing intensity in this region has been  
485 increasing in recent years. Nevertheless, it must be noted that the stocking rate threshold may exceed  
486 the carrying capacity, because it is predicted to lead to an extreme grassland degradation (Zhu et al.,  
487 2023a). The GDGI dataset also showed a similar pattern between the grazing intensity data and the  
488 WorldPop data near the built-up areas, indicating higher grazing intensity around settlements than other  
489 regions on the QTP. In addition, the GDGI dataset also indicate that from 1990 to 2020, although the  
490 grazing intensity of the Plateau has generally decreased, the hotspot areas for grazing activities have  
491 remained almost unchanged. This implies that these regions should be the focus of adaptive grassland  
492 management to effectively prevent grassland degradation, mainly based on the grass–livestock balance  
493 which varies by time and space.

494 Encouragingly, the GDGI dataset show that the grazing intensity for two-thirds of the entire QTP  
495 grassland decreased over the past 31 years, which is also consistent with other studies (Sun et al., 2021;  
496 Li et al., 2021). Recent decades of biodiversity protection, active restoration projects as well as  
497 management measures, such as nature reserves, grazing exclusion, part grazing ban combined with  
498 fencing enclosure, are believed to have driven these decrease (Deng et al., 2017; Li and Bennett, 2019).  
499 In addition, most grassland in the eastern Sanjiangyuan, the mid-eastern Changtang, and the northern  
500 foothills of the Himalayas, showed a significant decrease with grazing intensity (Figure 6e), indicating  
501 the importance of protected areas on preventing overstock and grassland degradation. Meanwhile, the  
502 GDGI maps also show that the grazing density varies greatly among protected areas, possibly owing to  
503 the difference in policy implementation. For instance, it can be seen from the GDGI maps that grazing  
504 intensity are increasing in some protected areas, especially several wetland nature reserves on the Zoige  
505 plateau (Figure 6e). Moreover, the average grazing intensity in all nature reserves on the QTP has  
506 overall increased from 1990 to 2020, although their increase rate is much lower than the non-protected  
507 areas (0.0125 SU/hm<sup>2</sup>·10a vs. 0.0304 SU/hm<sup>2</sup>·10a), which implies that grassland management in  
508 protected areas still needs to be strengthened on the QTP.

509 The grazing initiatives in alignment with the Sustainable Development Goals (SDGs) on the QTP  
510 can benefit from the GDGI dataset. Firstly, determination a reasonable stocking rate is vital to prevent  
511 overstocking of the pastures, which will possibly induce extreme grassland degradation (Zhu et al.,  
512 2023a). Stocking rate determination can be optimized by using our grazing intensity maps and the  
513 stocking rate threshold maps of the QTP. Secondly, the GDGI maps can contribute to strategic  
514 placement of fence, which is a common practice adopted to prevent grassland degradation on the QTP.  
515 Building fences in areas with high grazing intensity and exceeding the carrying capacity can improve  
516 the effectiveness of fence construction (Zhou et al., 2023; Zhang et al., 2023). Thirdly, the GDGI

517 dataset can provide a solid support for promoting effective nature reserve management, which in total  
518 covering nearly one third of the entire QTP. For example, the GDGI maps showed that grazing  
519 activities still exist in most nature reserves on the Plateau, although most of them have significantly  
520 lower grazing intensities compared with their adjacent non-protected areas. By using the GDGI maps,  
521 the conflict between ecological protection and grazing activities in nature reserves can be alleviated.  
522 Finally, our grazing intensity maps can act as a basic dataset to support other grassland-related policies.  
523 Currently, these policies on the QTP often adopt a one-size-fits-all approach to determine the carrying  
524 capacity and carry out ecological compensation, which may lead to overstock or unfair financial  
525 distribution (Wang et al., 2022). The grassland management strategies balancing carrying capacity and  
526 stocking rates are more likely to result in optimal management choices for policymakers and  
527 stakeholders, and our GDGI maps can contribute to this decision-making processes.

#### 528 **4.4 Uncertainties and limitations**

529 Although this study has collected as reliable datasets as possible, users of the GDGI products  
530 should be cognizant of inherent uncertainties and limitations within these datasets. Notably, the mean  
531 relative error of the GDGI dataset spanning 1990 to 2020 was recorded at 4.2% (Figure 4a), calculated  
532 from the average errors across 182 counties within the QTP that had accessible livestock census data.  
533 Furthermore, approximately 8.26% of grassland areas exhibited a relative error exceeding 1.0 SU/hm<sup>2</sup>  
534 (Figure 4b). Such discrepancies arise from several limitations that were subsequently propagated to the  
535 final grazing intensity maps, thereby contributing to the dataset's overall uncertainties.

536 Firstly, the estimations of grazing intensities were fundamentally conservative, primarily due to the  
537 lack of comprehensive input data. Livestock numbers, derived from year-end data at the county level,  
538 inadvertently led to underestimations of grazing intensity by not accounting for livestock off-take rates.  
539 Likewise, the evaluation focused solely on livestock grazing intensity, excluding wild herbivores and  
540 forage-dependent livestock, which potentially underestimate actual grazing pressures on the QTP.  
541 Additionally, despite identifying seven main factors influencing livestock distribution, the study did not  
542 encompass all potential factors, such as fencing, forage availability, road proximity, and season  
543 transformation in grazing practices. Moreover, to align with county-scale livestock census data, we  
544 averaged the environmental factors at the county-scale. Although this approach have been widely used  
545 on the hypothesis that a consistent causal relationship between livestock intensity and environmental  
546 factors persists across various scales (Robinson et al., 2014; Nicolas et al., 2016; Li et al., 2021; Meng  
547 et al., 2023), it might oversimplify the intricate dynamics between grazing intensity and lead to a  
548 certain degree of estimation inaccuracies. In addition, the reliance on linear extrapolation to  
549 Supplementary missing gridded 100-m population density data from 1990-1999 introduced further  
550 uncertainties due to the limited resolution (1-km) and interval (5-year) of the ChinaPop dataset.

551 Secondly, the modeling process for mapping grazing intensity also suffered from several challenges.  
552 Specifically, this study adopted the FAO's assumption that the relationship between environmental  
553 factors and livestock intensity is uniform across both administrative and pixel levels. However, it is  
554 unlikely that these relationships are entirely consistent across scales, and the county-level model's  
555 approach inevitably smooths spatial details, potentially reducing the precision of the data. Furthermore,  
556 the ET model was trained with a limited sample size of 4,998 and applied to a vast area consisting of  
557 150 million pixels, which could compromise the model's accuracy. In addition, despite the ET model's  
558 design to reduce overfitting risks by using randomly selected features and partition decision, the  
559 potential for overfit effects still remained, particularly when faced with a high number of output classes

560 or insufficient sample sizes (Geurts et al., 2006; Galelli and Castelletti, 2013). In fact, this limitation  
561 was evident in this study, as the generalization capability of the ET model was restricted by the  
562 disparity between the number of training samples and the total number of pixels, leading to predictions  
563 that often exceed actual livestock census (Figure 4a).

564 Thirdly, our methodological framework for high-resolution gridded grazing dataset mapping was  
565 developed based on the assumption that all grassland were accessible to livestock. However, in reality,  
566 the amount of available grassland was less due to fencing and grazing bans on the QTP (Zhan et al.,  
567 2023). Moreover, transhumant herders generally follow a seasonal calendar for summer pastures and  
568 winter pastures on the QTP. However, we did not consider this seasonal movements due to data  
569 limitations, which further restrict the analysis of seasonal livestock distribution patterns (Kolluru et al.,  
570 2023). Additionally, the model's reliance on human population as a proxy for livestock locations  
571 overlooked the possibility of high grazing intensity in areas with low human populations on the QTP,  
572 particularly in regions designated for summer pastures.

573 Finally, it is important to note that gathering livestock census data in the Qinghai-Tibet Plateau  
574 presents significant challenges, leading to a scarcity of livestock validation data in this study,  
575 particularly at the township and pixel scales. This limitation may, to some extent, impact the reliability  
576 of the grazing intensity data we have presented.

577 In summary, all these limitations associated with input data, the modeling process, and the  
578 methodological framework collectively contribute to the uncertainties and reduce accuracy of the  
579 GDGI maps. We henceforth recommend that future research should aim to incorporate more detailed  
580 data, consider additional influential factors, enhance key dataset's time-series consistency, and refine  
581 the methodological framework to improve the accuracy of grazing intensity mapping.

## 582 **5 Data availability**

583 The annual gridded grazing intensity maps of the QTP spanning from 1990 to 2020 are accessible  
584 at the following link: <https://doi.org/10.5281/zenodo.10851119> (Zhou et al., 2024). Each map is  
585 catalogued by year and recorded in GeoTIFF format, with values represented in SU/hm<sup>2</sup> per year.  
586 These datasets, with a spatial resolution of 100 m and annual temporal resolution, utilize the  
587 WGS-1984-Albers geographic coordinate system. To streamline data transfer and download processes,  
588 the comprehensive 31-year dataset has been compressed into a ZIP file, readily available for download  
589 and compatible with Geographic Information System (GIS) software for viewing.

## 590 **6 Conclusions**

591 In this study, we introduce a framework utilizing ET machine learning algorithms to achieve  
592 fine-scale livestock spatialization, subsequently generating the GDGI dataset across the QTP. The  
593 GDGI has a spatial resolution of 100 m and expands 31 years from 1990 to 2020. It is consistent with  
594 county livestock census data of the QTP, and the accuracy evaluations at both pixel-level and  
595 township-level underscore the outstanding reliability and applicability of the GDGI dataset, which can  
596 successfully capture the spatial heterogeneity and variation in grazing intensities in greater details.  
597 Moreover, comparisons between the GDGI dataset and other existing grazing map products further  
598 proved the robust and efficient of our dataset, and demonstrate the validity of the proposed framework  
599 in the research of livestock spatialization. Nonetheless, it is imperative for data users to recognize that  
600 the GDGI may still contain inherent uncertainties. Our Monte Carlo simulations have estimated the

601 average MRE for grazing intensity across the QTP to vary between 6.84% and 9.08%. The GDGI  
602 dataset, as presented in this study, can enhance the understanding of grazing activities on the QTP. This,  
603 in turn, can aid in the rational utilization of grasslands and facilitate the implementation of informed  
604 and sustainable management practices.

#### 605 **Supplementary.**

606 For gridded datasets influencing grazing that are not directly available, or that do not meet  
607 spatio-temporal resolution requirements—such as those pertaining to population density, temperature,  
608 precipitation, and HNPP—we have delineated the processing or creation procedures in the  
609 Supplementary file.

#### 610 **Author contributions.**

611 T.L. conceived the research; J.Z. and J.N. performed the analyses and wrote the first draft of the  
612 paper; N.W. and T.L. reviewed and edited the paper before submission. All authors made substantial  
613 contributions to the discussion of content.

#### 614 **Competing interests.**

615 The authors declare that they have no conflict of interest.

#### 616 **Acknowledgements.**

617 We would like to thank the Bureau of Statistics of each county over the QTP for providing the  
618 census livestock data.

#### 619 **Financial support.**

620 This research was supported by the Second Tibetan Plateau Scientific Expedition and Research  
621 Program (STEP), Ministry of Science and Technology of the People's Republic of China (grant no.  
622 2019QZKK0402) and the National Natural Science Foundation of China (grant no. 42071238).

#### 623 **References**

- 624 Abu Hammad, A. and Tumeizi, A.: Land degradation: socioeconomic and environmental causes and  
625 consequences in the eastern Mediterranean, *Land. Degrad. Dev.*, 23, 216-226,  
626 <https://doi.org/10.1002/ldr.1069>, 2012.
- 627 Ahmad, M. W., Reynolds, J., and Rezgui, Y.: Predictive modelling for solar thermal energy systems: A  
628 comparison of support vector regression, random forest, extra trees and regression trees, *J. Clean.*  
629 *Prod.*, 203, 810-821, <https://doi.org/10.1016/j.jclepro.2018.08.207>, 2018.
- 630 Alexander, P., Prestele, R., Verburg, P. H., Arneth, A., Baranzelli, C., Batista e Silva, F., Brown, C.,  
631 Butler, A., Calvin, K., and Dendoncker, N.: Assessing uncertainties in land cover projections, *Glob.*  
632 *Chang. Biol.*, 23, 767-781, 2017.
- 633 Allred, B. W., Fuhlendorf, S. D., Hovick, T. J., Dwayne Elmore, R., Engle, D. M., and Joern, A.:

634 Conservation implications of native and introduced ungulates in a changing climate, *Glob. Chang.*  
635 *Biol.*, 19, 1875-1883, <https://doi.org/10.1111/gcb.12183>, 2013.

636 Breiman, L.: Random Forests, *Mach. Learn.*, 45, 5-32, <https://doi.org/10.1023/A:1010933404324>,  
637 2001.

638 Cai, Y. J., Wang, X. D., Tian, L. L., Zhao, H., Lu, X. Y., and Yan, Y.: The impact of excretal returns  
639 from yak and Tibetan sheep dung on nitrous oxide emissions in an alpine steppe on the  
640 Qinghai-Tibetan Plateau, *Soil. Biol. Biochem.*, 76, 90-99,  
641 <https://doi.org/10.1016/j.soilbio.2014.05.008>, 2014.

642 Chang, J. F., Ciais, P., Gasser, T., Smith, P., Herrero, M., Havlík, P., Obersteiner, M., Guenet, B., Goll,  
643 D. S., Li, W., Naipal, V., Peng, S. S., Qiu, C. J., Tian, H. Q., Viovy, N., Yue, C., and Zhu, D.: Climate  
644 warming from managed grasslands cancels the cooling effect of carbon sinks in sparsely grazed and  
645 natural grasslands, *Nat. Commun.*, 12, 118, <https://doi.org/10.1038/s41467-020-20406-7>, 2021.

646 Chen, Y. Z., Ju, W. M., Mu, S. J., Fei, X. R., Cheng, Y., Propastin, P., Zhou, W., Liao, C. J., Chen, L. X.,  
647 Tang, R. J., Qi, J. G., Li, J. L., and Ruan, H. H.: Explicit Representation of Grazing Activity in a  
648 Diagnostic Terrestrial Model: A Data - Process Combined Scheme, *J. Adv. Model. Earth. Sy.*, 11,  
649 957-978, <https://doi.org/10.1029/2018ms001352>, 2019.

650 Cortes, C. and Vapnik, V.: Support-vector networks, *Mach. Learn.*, 20, 273-297,  
651 <https://doi.org/10.1007/BF00994018>, 1995.

652 Cover, T. and Hart, P.: Nearest neighbor pattern classification, *Ieee. T. Inform. Theory.*, 13, 21-27,  
653 <https://doi.org/10.1109/TIT.1967.1053964>, 1967.

654 Dara, A., Baumann, M., Freitag, M., Hölzel, N., Hostert, P., Kamp, J., Müller, D., Prishchepov, A. V.,  
655 and Kuemmerle, T.: Annual Landsat time series reveal post-Soviet changes in grazing pressure,  
656 *Remote. Sens. Environ.*, 239, 111667, <https://doi.org/10.1016/j.rse.2020.111667>, 2020.

657 Deng, L., Zhou, S. G., Wu, P., Gao, L., and Chang, X.: Effects of grazing exclusion on carbon  
658 sequestration in China's grassland, *Earth-Sci. Rev.*, 173, 84-95,  
659 <https://doi.org/10.1016/j.earscirev.2017.08.008>, 2017.

660 Dong, S. K., Shang, Z. H., Gao, J. X., and Boone, R. B.: Enhancing sustainability of grassland  
661 ecosystems through ecological restoration and grazing management in an era of climate change on  
662 Qinghai-Tibetan Plateau, *Agr. Ecosyst. Environ.*, 287, 106684,  
663 <https://doi.org/10.1016/j.agee.2019.106684>, 2020.

664 Fang, X. N. and Wu, J. G.: Causes of overgrazing in Inner Mongolian grasslands: Searching for deep  
665 leverage points of intervention, *Ecol. Soc.*, 27, <https://doi.org/10.5751/es-12878-270108>, 2022.

666 Feng, R. Z., Long, R. J., Shang, Z. H., Ma, Y. S., Dong, S. K., and Wang, Y. L.: Establishment of  
667 *Elymus natans* improves soil quality of a heavily degraded alpine meadow in Qinghai-Tibetan  
668 Plateau, China, *Plant. Soil.*, 327, 403-411, <https://doi.org/10.1007/s11104-009-0065-3>, 2009.

669 Fetzl, T., Havlik, P., Herrero, M., Kaplan, J. O., Kastner, T., Kroisleitner, C., Rolinski, S., Searchinger,  
670 T., Van Bodegom, P. M., Wirsén, S., and Erb, K. H.: Quantification of uncertainties in global  
671 grazing systems assessment, *Global. Biogeochem. Cy.*, 31, 1089-1102,  
672 <https://doi.org/10.1002/2016gb005601>, 2017.

673 Friedman, J. H.: Greedy function approximation: a gradient boosting machine, *Ann. Stat.*, 29,  
674 1189-1232, <https://doi.org/10.1214/aos/1013203451>, 2001.

675 Galelli, S. and Castelletti, A.: Assessing the predictive capability of randomized tree-based ensembles  
676 in streamflow modelling, *Hydrol. Earth. Syst. Sc.*, 17, 2669-2684,  
677 <https://doi.org/10.5194/hess-17-2669-2013>, 2013.

678 García, R., Aguilar, J., Toro, M., Pinto, A., and Rodríguez, P.: A systematic literature review on the use  
679 of machine learning in precision livestock farming, *Comput. Electron. Agr.*, 179, 105826,  
680 <https://doi.org/10.1016/j.compag.2020.105826>, 2020.

681 García Ruiz, J. M., Tomás Faci, G., Diarte Blasco, P., Montes, L., Domingo, R., Sebastián, M., Lasanta,  
682 T., González Sampériz, P., López Moreno, J. I., Arnáez, J., and Beguería, S.: Transhumance and  
683 long-term deforestation in the subalpine belt of the central Spanish Pyrenees: An interdisciplinary  
684 approach, *Catena.*, 195, 104744, <https://doi.org/10.1016/j.catena.2020.104744>, 2020.

685 Garrett, R. D., Koh, I., Lambin, E. F., le Polain de Waroux, Y., Kastens, J. H., and Brown, J. C.:  
686 Intensification in agriculture-forest frontiers: Land use responses to development and conservation  
687 policies in Brazil, *Global Environ. Chang.*, 53, 233-243,  
688 <https://doi.org/10.1016/j.gloenvcha.2018.09.011>, 2018.

689 Geurts, P., Ernst, D., and Wehenkel, L.: Extremely randomized trees, *Mach. Learn.*, 63, 3-42,  
690 <https://doi.org/10.1007/s10994-006-6226-1>, 2006.

691 Gilbert, M., Nicolas, G., Cinardi, G., Van Boeckel, T. P., Vanwambeke, S. O., Wint, G. R. W., and  
692 Robinson, T. P.: Global distribution data for cattle, buffaloes, horses, sheep, goats, pigs, chickens and  
693 ducks in 2010, *Sci. Data.*, 5, 180227, <https://doi.org/10.1038/sdata.2018.227>, 2018.

694 Godfray, H. C. J., Aveyard, P., Garnett, T., Hall, J. W., Key, T. J., Lorimer, J., Pierrehumbert, R. T.,  
695 Scarborough, P., Springmann, M., and Jebb, S. A.: Meat consumption, health, and the environment,  
696 *Science.*, 361, 243, <https://doi.org/10.1126/science.aam5324>, 2018.

697 Guo, Z. L., Li, Z., and Cui, G. F.: Effectiveness of national nature reserve network in representing  
698 natural vegetation in mainland China, *Biodivers. Conserv.*, 24, 2735-2750,  
699 <https://doi.org/10.1007/s10531-015-0959-8>, 2015.

700 Han, Y. H., Dong, S. K., Zhao, Z. Z., Sha, W., Li, S., Shen, H., Xiao, J. N., Zhang, J., Wu, X. Y., Jiang,  
701 X. M., Zhao, J. B., Liu, S. L., Dong, Q. M., Zhou, H. K., and Yeomans, J. C.: Response of soil  
702 nutrients and stoichiometry to elevated nitrogen deposition in alpine grassland on the  
703 Qinghai-Tibetan Plateau, *Geoderma.*, 343, 263-268, <https://doi.org/10.1016/j.geoderma.2018.12.050>,  
704 2019.

705 He, M., Pan, Y. H., Zhou, G. Y., Barry, K. E., Fu, Y. L., and Zhou, X. H.: Grazing and global change  
706 factors differentially affect biodiversity - ecosystem functioning relationships in grassland  
707 ecosystems, *Glob. Chang. Biol.*, 28, 5492-5504, <https://doi.org/10.1111/gcb.16305>, 2022.

708 Heddam, S., Ptak, M., and Zhu, S. L.: Modelling of daily lake surface water temperature from air  
709 temperature: Extremely randomized trees (ERT) versus Air2Water, MARS, M5Tree, RF and  
710 MLPNN, *J. Hydrol.*, 588, 125130, <https://doi.org/10.1016/j.jhydrol.2020.125130>, 2020.

711 Hu, Y., Cheng, H., and Tao, S.: Environmental and human health challenges of industrial livestock and  
712 poultry farming in China and their mitigation, *Environ. Int.*, 107, 111-130,  
713 <https://doi.org/10.1016/j.envint.2017.07.003>, 2017.

714 Huang, X. T., Yang, Y. S., Chen, C. B., Zhao, H. F., Yao, B. Q., Ma, Z., Ma, L., and Zhou, H. K.:  
715 Quantifying and Mapping Human Appropriation of Net Primary Productivity in Qinghai Grasslands  
716 in China, *Agriculture.*, 12, 483, <https://doi.org/10.3390/agriculture12040483>, 2022.

717 Humpenöder, F., Bodirsky, B. L., Weindl, I., Lotze Campen, H., Linder, T., and Popp, A.: Projected  
718 environmental benefits of replacing beef with microbial protein, *Nature.*, 605, 90-96,  
719 <https://doi.org/10.1038/s41586-022-04629-w>, 2022.

720 Jiang, M. J., Zhao, X. F., Wang, R., Yin, L., and Zhang, B. L.: Assessment of Conservation  
721 Effectiveness of the Qinghai-Tibet Plateau Nature Reserves from a Human Footprint Perspective



722 with Global Lessons, *Land.*, 12, 869, <https://doi.org/10.3390/land12040869>, 2023.

723 Kolluru, V., John, R., Saraf, S., Chen, J. Q., Hankerson, B., Robinson, S., Kussainova, M., and Jain, K.:  
724 Gridded livestock density database and spatial trends for Kazakhstan, *Sci. Data.*, 10, 839,  
725 <https://doi.org/10.1038/s41597-023-02736-5>, 2023.

726 Kumar, P., Abubakar, A. A., Verma, A. K., Umaraw, P., Adewale Ahmed, M., Mehta, N., Nizam Hayat,  
727 M., Kaka, U., and Sazili, A. Q.: New insights in improving sustainability in meat production:  
728 opportunities and challenges, *Crit .Rev. Food. Sci.*, 1-29,  
729 <https://doi.org/10.1080/10408398.2022.2096562>, 2022.

730 Li, M. Q., Liu, S. L., Wang, F. F., Liu, H., Liu, Y. X., and Wang, Q. B.: Cost-benefit analysis of  
731 ecological restoration based on land use scenario simulation and ecosystem service on the  
732 Qinghai-Tibet Plateau, *Glob. Ecol. Conserv.*, 34, e02006,  
733 <https://doi.org/10.1016/j.gecco.2022.e02006>, 2022a.

734 Li, P. and Bennett, J.: Understanding herders' stocking rate decisions in response to policy initiatives,  
735 *Sci. Total. Environ.*, 672, 141-149, <https://doi.org/10.1016/j.scitotenv.2019.03.407>, 2019.

736 Li, Q., Zhang, C. L., Shen, Y. P., Jia, W. R., and Li, J.: Quantitative assessment of the relative roles of  
737 climate change and human activities in desertification processes on the Qinghai-Tibet Plateau based  
738 on net primary productivity, *Catena.*, 147, 789-796, <https://doi.org/10.1016/j.catena.2016.09.005>,  
739 2016.

740 Li, S., Wu, J., Gong, J., and Li, S.: Human footprint in Tibet: Assessing the spatial layout and  
741 effectiveness of nature reserves, *Sci Total Environ*, 621, 18-29,  
742 <https://doi.org/10.1016/j.scitotenv.2017.11.216>, 2018.

743 Li, T., Cai, S. H., Singh, R. K., Cui, L. Z., Fava, F., Tang, L., Xu, Z. H., Li, C. J., Cui, X. Y., Du, J. Q.,  
744 Hao, Y. B., Liu, Y. X., and Wang, Y. F.: Livelihood resilience in pastoral communities:  
745 Methodological and field insights from Qinghai-Tibetan Plateau, *Sci. Total. Environ.*, 838, 155960,  
746 <https://doi.org/10.1016/j.scitotenv.2022.155960>, 2022b.

747 Li, X. H., Hou, J. L., and Huang, C. L.: High-Resolution Gridded Livestock Projection for Western  
748 China Based on Machine Learning, *Remote. Sens.*, 13, 5038, <https://doi.org/10.3390/rs13245038>,  
749 2021.

750 Lin, G. C., Lin, A. J., and Gu, D. L.: Using support vector regression and K-nearest neighbors for  
751 short-term traffic flow prediction based on maximal information coefficient, *Inform. Sciences.*, 608,  
752 517-531, <https://doi.org/10.1016/j.ins.2022.06.090>, 2022.

753 Liu, B. T.: Actual livestock carrying capacity estimation product in Qinghai-Tibet Plateau (2000-2019),  
754 National Tibetan Plateau Data Center. [Dataset], <https://doi.org/10.11888/Ecolo.tpd.271513>,  
755 2021.

756 Long, S. J., Wei, X. L., Zhang, F., Zhang, R. H., Xu, J., Wu, K., Li, Q. Q., and Li, W. W.: Estimating  
757 daily ground-level NO<sub>2</sub> concentrations over China based on TROPOMI observations and machine  
758 learning approach, *Atmos. Environ.*, 289, 119310, <https://doi.org/10.1016/j.atmosenv.2022.119310>,  
759 2022.

760 Luo, J. F., Hoogendoorn, C., van der Weerden, T., Saggart, S., de Klein, C., Giltrap, D., Rollo, M., and  
761 Rys, G.: Nitrous oxide emissions from grazed hill land in New Zealand, *Agr. Ecosyst. Environ.*, 181,  
762 58-68, <https://doi.org/10.1016/j.agee.2013.09.020>, 2013.

763 Ma, C., Xie, Y., Duan, H., Wang, X., Bie, Q., Guo, Z., He, L., and Qin, W.: Spatial quantification  
764 method of grassland utilization intensity on the Qinghai-Tibetan Plateau: A case study on the Selinco  
765 basin, *J. Environ. Manage.*, 302, 114073, <https://doi.org/10.1016/j.jenvman.2021.114073>, 2022.

766 Mack, G., Walter, T., and Flury, C.: Seasonal alpine grazing trends in Switzerland: Economic  
767 importance and impact on biotic communities, *Environ. Sci. Policy.*, 32, 48-57,  
768 <https://doi.org/10.1016/j.envsci.2013.01.019>, 2013.

769 Martinuzzi, S., Radeloff, V. C., Pastur, G. M., Rosas, Y. M., Lizarraga, L., Politi, N., Rivera, L., Herrera,  
770 A. H., Silveira, E. M. O., Olah, A., and Pidgeon, A. M.: Informing forest conservation planning with  
771 detailed human footprint data for Argentina, *Glob. Ecol. Conserv.*, 31, e01787,  
772 <https://doi.org/10.1016/j.gecco.2021.e01787>, 2021.

773 McMillan, H. K., Westerberg, I. K., and Krueger, T.: Hydrological data uncertainty and its implications,  
774 *Wiley Interdisciplinary Reviews: Water*, 5, e1319, 2018.

775 McSherry, M. E. and Ritchie, M. E.: Effects of grazing on grassland soil carbon: a global review, *Glob.*  
776 *Chang. Biol.*, 19, 1347-1357, <https://doi.org/10.1111/gcb.12144>, 2013.

777 Meng, N., Wang, L. J., Qi, W. C., Dai, X. H., Li, Z. Z., Yang, Y. Z., Li, R. N., Ma, J. F., and Zheng, H.:  
778 A high-resolution gridded grazing dataset of grassland ecosystem on the Qinghai-Tibet Plateau in  
779 1982-2015, *Sci. Data.*, 10, 68, <https://doi.org/10.1038/s41597-023-01970-1>, 2023.

780 Miao, L. J., Sun, Z. L., Ren, Y. J., Schierhorn, F., and Müller, D.: Grassland greening on the Mongolian  
781 Plateau despite higher grazing intensity, *Land. Degrad. Dev.*, 32, 792-802,  
782 <https://doi.org/10.1002/ldr.3767>, 2020.

783 Minoofar, A., Gholami, A., Eslami, S., Hajizadeh, A., Gholami, A., Zandi, M., Ameri, M., and Kazem,  
784 H. A.: Renewable energy system opportunities: A sustainable solution toward cleaner production and  
785 reducing carbon footprint of large-scale dairy farms, *Energ. Convers. Manage.*, 293, 117554,  
786 <https://doi.org/10.1016/j.enconman.2023.117554>, 2023.

787 Mulligan, M., van Soesbergen, A., Hole, D. G., Brooks, T. M., Burke, S., and Hutton, J.: Mapping  
788 nature's contribution to SDG 6 and implications for other SDGs at policy relevant scales, *Remote.*  
789 *Sens. Environ.*, 239, 111671, <https://doi.org/10.1016/j.rse.2020.111671>, 2020.

790 Muloi, D. M., Wee, B. A., McClean, D. M. H., Ward, M. J., Pankhurst, L., Phan, H., Ivens, A. C.,  
791 Kivali, V., Kiyong'a, A., Ndinda, C., Gitahi, N., Ouko, T., Hassell, J. M., Imboma, T., Akoko, J.,  
792 Murungi, M. K., Njoroge, S. M., Muinde, P., Nakamura, Y., Alumasa, L., Furmaga, E., Kaitho, T.,  
793 Öhgren, E. M., Amany, F., Ogendo, A., Wilson, D. J., Bettridge, J. M., Kiiru, J., Kyobutungi, C.,  
794 Tacoli, C., Kang'ethe, E. K., Davila, J. D., Kariuki, S., Robinson, T. P., Rushton, J., Woolhouse, M. E.  
795 J., and Fèvre, E. M.: Population genomics of *Escherichia coli* in livestock-keeping households across  
796 a rapidly developing urban landscape, *Nat. Microbiol.*, 7, 581-589,  
797 <https://doi.org/10.1038/s41564-022-01079-y>, 2022.

798 Neumann, K., Elbersen, B. S., Verburg, P. H., Staritsky, I., Pérez-Soba, M., de Vries, W., and Rienks, W.  
799 A.: Modelling the spatial distribution of livestock in Europe, *Landscape. Ecol.*, 24, 1207-1222,  
800 <https://doi.org/10.1007/s10980-009-9357-5>, 2009.

801 Nicolas, G., Robinson, T. P., Wint, G. R., Conchedda, G., Cinardi, G., and Gilbert, M.: Using Random  
802 Forest to Improve the Downscaling of Global Livestock Census Data, *Plos. One.*, 11, e0150424,  
803 <https://doi.org/10.1371/journal.pone.0150424>, 2016.

804 O'Neill, D. W. and Abson, D. J.: To settle or protect? A global analysis of net primary production in  
805 parks and urban areas, *Ecol. Econ.*, 69, 319-327, <https://doi.org/10.1016/j.ecolecon.2009.08.028>,  
806 2009.

807 Pan, Y. J., Chen, S. Y., Qiao, F. X., Ukkusuri, S. V., and Tang, K.: Estimation of real-driving emissions  
808 for buses fueled with liquefied natural gas based on gradient boosted regression trees, *Sci. Total.*  
809 *Environ.*, 660, 741-750, <https://doi.org/10.1016/j.scitotenv.2019.01.054>, 2019.

810 Petz, K., Alkemade, R., Bakkenes, M., Schulp, C. J. E., van der Velde, M., and Leemans, R.: Mapping  
811 and modelling trade-offs and synergies between grazing intensity and ecosystem services in  
812 rangelands using global-scale datasets and models, *Global. Environ. Chang.*, 29, 223-234,  
813 <https://doi.org/10.1016/j.gloenvcha.2014.08.007>, 2014.

814 Pozo, R. A., Cusack, J. J., Acebes, P., Malo, J. E., Traba, J., Iranzo, E. C., Morris-Trainor, Z.,  
815 Minderman, J., Bunnefeld, N., Radic-Schilling, S., Moraga, C. A., Arriagada, R., and Corti, P.:  
816 Reconciling livestock production and wild herbivore conservation: challenges and opportunities,  
817 *Trends. Ecol. Evol.*, 36, 750-761, <https://doi.org/10.1016/j.tree.2021.05.002>, 2021.

818 Prosser, D. J., Wu, J., Ellis, E. C., Gale, F., Van Boeckel, T. P., Wint, W., Robinson, T., Xiao, X., and  
819 Gilbert, M.: Modelling the distribution of chickens, ducks, and geese in China, *Agric Ecosyst*  
820 *Environ*, 141, 381-389, <https://doi.org/10.1016/j.agee.2011.04.002>, 2011.

821 Robinson, T. P., Wint, G. R., Conchedda, G., Van Boeckel, T. P., Ercoli, V., Palamara, E., Cinardi, G.,  
822 D'Aietti, L., Hay, S. I., and Gilbert, M.: Mapping the global distribution of livestock, *Plos. One.*, 9,  
823 e96084, <https://doi.org/10.1371/journal.pone.0096084>, 2014.

824 Rokach, L.: Decision forest: Twenty years of research, *Inform. Fusion.*, 27, 111-125,  
825 <https://doi.org/10.1016/j.inffus.2015.06.005>, 2016.

826 Shakoor, A., Shakoor, S., Rehman, A., Ashraf, F., Abdullah, M., Shahzad, S. M., Farooq, T. H., Ashraf,  
827 M., Manzoor, M. A., Altaf, M. M., and Altaf, M. A.: Effect of animal manure, crop type, climate  
828 zone, and soil attributes on greenhouse gas emissions from agricultural soils-A global meta-analysis,  
829 *J. Clean. Prod.*, 278, 124019, <https://doi.org/10.1016/j.jclepro.2020.124019>, 2021.

830 Sun, J., Liu, M., Fu, B. J., Kemp, D., Zhao, W. W., Liu, G. H., Han, G. D., Wilkes, A., Lu, X. Y., Chen,  
831 Y. C., Cheng, G. W., Zhou, T. C., Hou, G., Zhan, T. Y., Peng, F., Shang, H., Xu, M., Shi, P. L., He, Y.  
832 T., Li, M., Wang, J. N., Tsunekawa, A., Zhou, H. K., Liu, Y., Li, Y. R., and Liu, S. L.: Reconsidering  
833 the efficiency of grazing exclusion using fences on the Tibetan Plateau, *Sci. Bull.*, 65, 1405-1414,  
834 <https://doi.org/10.1016/j.scib.2020.04.035>, 2020.

835 Sun, Y. X., Liu, S. L., Liu, Y. X., Dong, Y. H., Li, M. Q., An, Y., and Shi, F. N.: Grazing intensity and  
836 human activity intensity data sets on the Qinghai - Tibetan Plateau during 1990 - 2015, *Geoscience.*  
837 *Data. Journal*, 9, 140-153, <https://doi.org/10.1002/gdj3.127>, 2021.

838 Tabassum, A., Abbasi, T., and Abbasi, S. A.: Reducing the global environmental impact of livestock  
839 production: the minilivestock option, *J. Clean. Prod.*, 112, 1754-1766,  
840 <https://doi.org/10.1016/j.jclepro.2015.02.094>, 2016.

841 Van Boeckel, T. P., Prosser, D., Franceschini, G., Biradar, C., Wint, W., Robinson, T., and Gilbert, M.:  
842 Modelling the distribution of domestic ducks in Monsoon Asia, *Agr. Ecosyst. Environ.*, 141, 373-380,  
843 <https://doi.org/10.1016/j.agee.2011.04.013>, 2011.

844 Veldhuis, M. P., Ritchie, M. E., Ogutu, J. O., Morrison, T. A., Beale, C. M., Estes, A. B., Mwakilema,  
845 W., Ojwang, G. O., Parr, C. L., Probert, J., Wargute, P. W., Hopcraft, J. G. C., and Han, O.:  
846 Cross-boundary human impacts compromise the Serengeti-Mara ecosystem, *Science.*, 363,  
847 1424-1428, <https://doi.org/10.1126/science.aav0564>, 2019.

848 Venglovsky, J., Sasakova, N., and Placha, I.: Pathogens and antibiotic residues in animal manures and  
849 hygienic and ecological risks related to subsequent land application, *Bioresour. Technol.*, 100,  
850 5386-5391, <https://doi.org/10.1016/j.biortech.2009.03.068>, 2009.

851 Waha, K., van Wijk, M. T., Fritz, S., See, L., Thornton, P. K., Wichern, J., and Herrero, M.: Agricultural  
852 diversification as an important strategy for achieving food security in Africa, *Glob. Chang. Biol.*, 24,  
853 3390-3400, <https://doi.org/10.1111/gcb.14158>, 2018.

854 Wang, R. J., Feng, Q. S., Jin, Z. R., and Liang, T. G.: The Restoration Potential of the Grasslands on the  
855 Tibetan Plateau, *Remote. Sens.*, 14, 80, <https://doi.org/10.3390/rs14010080>, 2021.

856 Wang, Y. F., Lv, W. W., Xue, K., Wang, S. P., Zhang, L. R., Hu, R. H., Zeng, H., Xu, X. L., Li, Y. M.,  
857 Jiang, L. L., Hao, Y. B., Du, J. Q., Sun, J. P., Dorji, T., Piao, S. L., Wang, C. H., Luo, C. Y., Zhang, Z.  
858 H., Chang, X. F., Zhang, M. M., Hu, Y. G., Wu, T. H., Wang, J. Z., Li, B. W., Liu, P. P., Zhou, Y.,  
859 Wang, A., Dong, S. K., Zhang, X. Z., Gao, Q. Z., Zhou, H. K., Shen, M. G., Wilkes, A., Mieke, G.,  
860 Zhao, X. Q., and Niu, H. S.: Grassland changes and adaptive management on the Qinghai–Tibetan  
861 Plateau, *Nat. Rev. Earth. Env.*, 3, 668-683, <https://doi.org/10.1038/s43017-022-00330-8>, 2022.

862 Wang, Y. X., Sun, Y., Wang, Z. F., Chang, S. H., and Hou, F. J.: Grazing management options for  
863 restoration of alpine grasslands on the Qinghai - Tibet Plateau, *Ecosphere.*, 9, e02515,  
864 <https://doi.org/10.1002/ecs2.2515>, 2018.

865 Wei, Y. Q., Lu, H. Y., Wang, J. N., Wang, X. F., and Sun, J.: Dual Influence of Climate Change and  
866 Anthropogenic Activities on the Spatiotemporal Vegetation Dynamics Over the Qinghai-Tibetan  
867 Plateau From 1981 to 2015, *Earth's Future.*, 10, 1-23, <https://doi.org/10.1029/2021EF002566>, 2022.

868 Yang, J. and Huang, X.: The 30 m annual land cover dataset and its dynamics in China from 1990 to  
869 2019, *Earth. Syst. Sci. Data.*, 13, 3907-3925, <https://doi.org/10.5194/essd-13-3907-2021>, 2021.

870 Yang, Y. J., Song, G., and Lu, S.: Assessment of land ecosystem health with Monte Carlo simulation: A  
871 case study in Qiqihaer, China, *J. Clean. Prod.*, 250, 119522, 2020.

872 Ye, T., Liu, W. H., Mu, Q. Y., Zong, S., Li, Y. J., and Shi, P. J.: Quantifying livestock vulnerability to  
873 snow disasters in the Tibetan Plateau: Comparing different modeling techniques for prediction,  
874 *International Journal of Disaster Risk Reduction*, 48, <https://doi.org/10.1016/j.ijdr.2020.101578>,  
875 2020.

876 Zhai, D. C., Gao, X. Z., Li, B. L., Yuan, Y. C., Jiang, Y. H., Liu, Y., Li, Y., Li, R., Liu, W., and Xu, J.:  
877 Driving Climatic Factors at Critical Plant Developmental Stages for Qinghai–Tibet Plateau Alpine  
878 Grassland Productivity, *Remote. Sens.*, 14, 1564, <https://doi.org/10.3390/rs14071564>, 2022.

879 Zhan, N., Liu, W. H., Ye, T., Li, H. D., Chen, S., and Ma, H.: High-resolution livestock seasonal  
880 distribution data on the Qinghai-Tibet Plateau in 2020, *Sci. Data.*, 10, 142,  
881 <https://doi.org/10.1038/s41597-023-02050-0>, 2023.

882 Zhang, B. H., Zhang, Y. L., Wang, Z. F., Ding, M. J., Liu, L. S., Li, L. H., Li, S. C., Liu, Q. H., Paudel,  
883 B., and Zhang, H. M.: Factors Driving Changes in Vegetation in Mt. Qomolangma (Everest):  
884 Implications for the Management of Protected Areas, *Remote. Sens.*, 13, 4725,  
885 <https://doi.org/10.3390/rs13224725>, 2021a.

886 Zhang, R. Y., Wang, Z. W., Han, G. D., Schellenberg, M. P., Wu, Q., and Gu, C.: Grazing induced  
887 changes in plant diversity is a critical factor controlling grassland productivity in the Desert Steppe,  
888 Northern China, *Agr. Ecosyst. Environ.*, 265, 73-83, <https://doi.org/10.1016/j.agee.2018.05.014>,  
889 2018.

890 Zhang, W. B., Li, J., Struik, P. C., Jin, K., Ji, B. M., Jiang, S. Y., Zhang, Y., Li, Y. H., Yang, X. J., and  
891 Wang, Z.: Recovery through proper grazing exclusion promotes the carbon cycle and increases  
892 carbon sequestration in semiarid steppe, *Sci. Total. Environ.*, 892, 164423,  
893 <https://doi.org/10.1016/j.scitotenv.2023.164423>, 2023.

894 Zhang, Y., Hu, Q. W., and Zou, F. L.: Spatio-Temporal Changes of Vegetation Net Primary Productivity  
895 and Its Driving Factors on the Qinghai-Tibetan Plateau from 2001 to 2017, *Remote. Sens.*, 13, 1566,  
896 <https://doi.org/10.3390/rs13081566>, 2021b.

897 Zhao, X. Q., Xu, T. W., Ellis, J., He, F. Q., Hu, L. Y., and Li, Q.: Rewilding the wildlife in

898 Sangjiangyuan National Park, Qinghai-Tibetan Plateau, *Ecosyst. Health. Sust.*, 6, 1776643,  
899 <https://doi.org/10.1080/20964129.2020.1776643>, 2020.

900 Zhou, W. X., Li, C. J., Wang, S., Ren, Z. B., and Stringer, L. C.: Effects of grazing and enclosure  
901 management on soil physical and chemical properties vary with aridity in China's drylands, *Sci.*  
902 *Total. Environ.*, 877, 162946, <https://doi.org/10.1016/j.scitotenv.2023.162946>, 2023.

903 Zhu, Q., Chen, H., Peng, C. H., Liu, J. X., Piao, S., He, J. S., Wang, S. P., Zhao, X. Q., Zhang, J., Fang,  
904 X. Q., Jin, J. X., Yang, Q. E., Ren, L. L., and Wang, Y. F.: An early warning signal for grassland  
905 degradation on the Qinghai-Tibetan Plateau, *Nat. Commun.*, 14, 6406,  
906 <https://doi.org/10.1038/s41467-023-42099-4>, 2023a.

907 Zhu, Y. Y., Zhang, H. M., Ding, M. J., Li, L. H., and Zhang, Y. L.: The Multiple Perspective Response  
908 of Vegetation to Drought on the Qinghai-Tibetan Plateau, *Remote. Sens.*, 15, 902,  
909 <https://doi.org/10.3390/rs15040902>, 2023b.

910 Zhou, J., Niu, J., Wu, N., Lu, T. Annual high-resolution grazing intensity maps on the Qinghai-Tibet  
911 Plateau from 1990 to 2020 [Dataset]. Zenodo. <https://doi.org/10.5281/zenodo.10851119>, 2024.